

1-1-1984

Study of the origin of Mexican Indian potshards by means of neutron activation analysis

Rafat M. Nassar
Iowa State University

Follow this and additional works at: <https://lib.dr.iastate.edu/rtd>

 Part of the [Engineering Commons](#)

Recommended Citation

Nassar, Rafat M., "Study of the origin of Mexican Indian potshards by means of neutron activation analysis" (1984). *Retrospective Theses and Dissertations*. 18523.
<https://lib.dr.iastate.edu/rtd/18523>

This Thesis is brought to you for free and open access by the Iowa State University Capstones, Theses and Dissertations at Iowa State University Digital Repository. It has been accepted for inclusion in Retrospective Theses and Dissertations by an authorized administrator of Iowa State University Digital Repository. For more information, please contact digirep@iastate.edu.

Study of the origin of Mexican Indian potshards
by means of neutron activation analysis

by

Rafat M. Nassar

A Thesis Submitted to the
Graduate Faculty in Partial Fulfillment of the
Requirements for the Degree of
MASTER OF SCIENCE

Major: Nuclear Engineering

Signatures have been redacted for privacy

Iowa State University
Ames, Iowa

1984

TABLE OF CONTENTS

	Page
1. INTRODUCTION	1
1.1. Technical Analysis of Pottery	1
1.2. Neutron Activation Analysis	4
1.3. Studies of Mesoamerican Pottery	13
1.4. Samples Description and Origin	14
1.4.1. Samples from Santa Cruz Acalpíxca, Xachimilco	16
1.4.2. Samples from Campeche	16
1.4.3. Samples from Chiapa de Corzo, Chiapas	16
2. EXPERIMENTAL PROCEDURE	18
2.1. Sampling, Encapsulation, and Irradiation	18
2.2. Standardization	19
2.3. Gamma Ray Detection	19
2.4. Spectrum Analysis and Determination of Trace- Element Concentrations	20
2.5. Discussion of Experimental Procedure	25
3. RESULTS AND DISCUSSION	36
3.1. Theory of Grouping Procedures	36
3.1.1. Cluster Analysis	36
3.1.2. Group Refinement	42
3.2. Formation of Groups	43
4. CONCLUSIONS	62
4.1. Archaeological Implications	62
4.2. Direction for Future Work	63
5. REFERENCES	64
6. ACKNOWLEDGEMENTS	68

LIST OF FIGURES

	Page
Figure 1. Gamma-ray spectra of sample [X-DR] obtained from activation measurements made five (Figure 1a) and seventeen (Figure 1b) days after irradiation, respectively	7
Figure 2. Map illustrating location from which samples were excavated	15
Figure 3. Sample changer detector system connection	21
Figure 4. Spectrum analysis and trace element determination flowchart	23
Figure 5. Dendogram resulting from centroid method	41
Figure 6. Dendogram resulting from average linkage method	44
Figure 7. Dendogram resulting from Ward's method	45
Figure 8. Relative concentration curves for samples 10, 11, 14, and DR	46
Figure 9. Relative concentration curves for sample 7, 8, 8b, 9, 12, 13, and 14 with respect to sample 11	49
Figure 10. Relative concentration curves for samples 8 and 8b	50
Figure 11. Relative concentration curves for samples 7 and 9	51
Figure 12. Relative concentration curves for samples 7, 8, 8b, and 9	53
Figure 13a. Relative concentration curves for sample 13 compared to the concentration range of the C group	55
Figure 13b. Relative concentration curves for sample 13 compared to samples 7, 8, 8b, and 9 (group C)	56
Figure 14a. Relative concentration curves for sample 12 compared to concentration average of the C group	57

LIST OF TABLES

	Page
Table 1. Element concentration in NBS-1633a fly ash	26
Table 2. Element concentration in the unknown samples	28
Table 3a. Gamma counted element five days after irradiation	33
Table 3b. Gamma counted elements twenty one days after irradiation	34
Table 4. The common elements between samples 8 and 8b and samples 7 and 9, respectively	52
Table 5. Mean concentration of 7, 8, 8b, and 9—Xachimilco collection	54

Figure 14b. Relative concentration curves for sample 12 compared to samples 7, 8, 8b, and 9 (group C)	58
Figure 15a. Relative concentration curves for sample 19 compared to the concentration range of the group C	60
Figure 15b. Relative concentration curves for sample 19 compared to samples 7, 8, 8b, and 9 (group C)	61

1. INTRODUCTION

1.1. Technical Analysis of Pottery

The determination of the provenance of artifacts, especially pottery, is an important aspect of archaeology. The appearance of pottery collections at a large number of contiguous sites gives information about their homelands. When the same style is found far from its homeland, this indicates some form of trade, but when it is found that the styles in a given region are suddenly altered, archaeologists can say that a new people has taken dominion.

Therefore, archaeologists have evolved over the years an elaborate system of classification based largely upon form and decorative style; all pottery unearthed is subjected to this typological analysis. However, this method of sourcing has its faults, particularly in regions where pottery of the same type was made at a number of different centers in a manner so uniform that stylistic criteria are deficient guides to origin [4]. A method not depending on the style of pots or the habits of potters and painters but on characteristics of the fabric of the pot, would permit archaeologists to make more definite statements about pot provenance.

Clays everywhere are composed of roughly the same main constituents, kaolinite, illite, and montmorillonite [14]. The characterization of a particular clay bed requires a study of an array of elements making up (comprising) the constituents of the clay. "Essentially, this is a matter of 'fingerprinting' for which one is not concerned with any specific element but rather with an array providing a pattern which

varies in a sensitive manner. This sensitivity must be provided by the trace elements because the major constituents are few in number" [31]. The determination of the concentrations of the minor constituents or elements in clay beds can establish a trace element pattern unique to a specific area. This pattern can be compared with corresponding patterns of pieces of pottery [32]. Obviously, if more elements are determined, the more positive will be the assignment of the connection between potshards and clay beds, since the probability of coincidental similarities in trace element patterns becomes very small.

This methodology has implicit assumptions: the first is that the raw clay was not transported over great distances for the manufacture of pots. This assumption is based on observations of modern day primitive potters. The second assumption is that the trace element concentration pattern remains unchanged both during manufacture of the pot and during the time the pot was buried underground.

In the case of manufacturing, addition of a temper (usually quite pure) will lower the concentration of all elements by a constant factor but leave the pattern of relative concentration unaltered. On the other hand, refinement of clay by allowing the larger grains to settle out will increase the trace element concentrations by a constant factor, once more leaving the pattern unchanged. In the case of firing, it was found that whenever raw clay and fired pottery from the same source have been compared, conformity for all elements except the volatile ones (KBr, SiO₂ and Ca) is notably good [1,11,32].

In the burial period, the effect of ground water percolation is serious on elements in soluble forms. A study [8] indicated that under

certain conditions barium concentrations may change between raw clay and excavated potshards, whereas most other elements remain constant for use as indicators of provenance.

Keeping these caveats in mind, similarity and, hence, provenance determination of pottery by means of neutron activation analysis can and usually does succeed.

The earliest attempts in ancient materials analysis by neutron activation analysis were severely handicapped because the equipment was relatively primitive. Initially, relatively few elements were determined, identified, and separated mainly on the basis of their decay rate. In the late fifties, however, gamma-ray spectroscopy improved due to the general availability of sodium-iodide scintillation detectors, energy scanning, and multichannel analyzers [41]. Now a small number of elements could be determined simultaneously without chemical separation but, due to the relatively poor resolution provided by these scintillation detectors, certain photopeaks from different radionuclides interfered with one another. Hence, if interference occurs, such photopeak measurements could not reveal accurately the concentration of all, or perhaps any, of the elements which composed the sample. The determination is easily made free of interference at some time in the decay process; e.g., a long-lived radionuclide would eventually be free of interference from the peaks attributed to short-lived radionuclides.

In the sixties, the introduction of the high resolution semiconductor diode detectors (lithium-drifted germanium and silicon detectors) revolutionized the neutron activation examination of ancient materials. It was now possible to separate close lying photopeaks

arising from different elements or from complex mixtures of elements and measure these activities. These new detectors were used in the study of pottery by Perlman and Asaro [32] and many others.

Neutron activation technique is based on the fact that numerous elements, when bombarded with neutrons (usually in a reactor), produce radioisotopes which emit gamma-rays of known energies, distinctive of those specific isotopes. Now, by measuring the number of gamma-rays of specific energies emitted by a sample of unknown composition, it is possible to calculate the concentrations of definite elements in the sample. The availability of nuclear reactors and large lithium-drifted germanium detectors have made pottery neutron activation analysis the most accurate method available for provenance studies.

1.2. Neutron Activation Analysis

The most common nuclear reaction employed in neutron activation analysis is the neutron-gamma (n,γ), in which a thermal neutron is captured by target atom and one or more gamma-rays are emitted promptly. The target atom remains unchanged as far as chemical identity is concerned; however, the nucleus-mass will increase by one mass unit. This new nucleus is usually unstable; therefore, it undergoes radioactive decay at a rate dependent on its nuclear nature. This decay may take many forms: β^- or β^+ particle emission followed by a gamma-ray emission; photon emission as a result of capture of an orbital electron. In either case, these photons are monoenergetic and characteristic of the nucleus which emits them. Thus, the detection of these photons is an indication of the presence of that nucleus in a sample. Also, the intensity of

these photons is proportional to the abundance of the source nucleus.

The amount of activity produced in a sample depends on several factors: the intensity of the neutron source (the neutron flux), the time duration of exposure, the neutron-capture cross-section, and the number of nuclei present in the sample. The neutron source can be a nuclear reactor, radioactive source Cf^{252} , electron and ion accelerators which produce high energy neutrons by (γ, n) , $D(d, n)$ or $T(d, n)$ reactions [3], but usually nuclear reactors are used because they produce very high neutron fluxes. The irradiation time can vary from seconds to several weeks.

The rate of decay of a radioactive nucleus is expressed in terms of half-life, or the amount of time required for half the total number of radioactive nuclei to decay. Half-lives of different radioactive nuclei range from fractions of a second to many years. The fact that atoms with short half-lives decay faster than those with long half-lives implies the importance of the time which elapses between neutron bombardment and the activity measurement, and that strong radiation from short-lived nuclei will initially mask weak radiation from the long-lived ones. Occasionally, a nucleus with an inconveniently short half-life can still be determined if it decays to another radioactive nucleus with a longer half-life; e.g., thorium-232, which when neutron activated to thorium-233, decays with a half-life of 22 minutes, to protactinium-233. The Pa^{233} , which has a half-life of 27 days, decays to uranium-233 or U^{233} . Another example, the U^{239} concentration is determined by Np^{239} decay measurements.

The mathematical expression that relates the various factors affecting the decay rate can be expressed by [26]:

$$A_0 = \phi \sigma N (1 - e^{-\lambda t_i})$$

where

A_0 = disintegration rate (in disintegrations per second) of the induced radionuclei at the end of the irradiation.

ϕ = neutron flux, in neutrons per cm^2 per second.

σ = neutron-capture cross-section of the target element in cm^2 .

N = Number of atoms of element irradiated.

$\lambda = \frac{\ln 2}{T_{1/2}}$ = decay constant of activated element, per second.

$T_{1/2}$ = half life for the isotope, sec.

t_i = irradiation time, in seconds.

Gamma-ray spectroscopy for complex spectra is most conveniently accomplished using a lithium-drifted germanium detector [25]. The passage of gamma-ray through the detector crystal forms charge carriers (holes and electrons). These charge carriers under the applied high electric field sweep to the opposite faces of the crystal. This collection process results in a small current pulse with magnitude proportional to the energy of the gamma-ray absorbed by the crystal. After collection, these pulses are amplified and sorted according to their size, resulting in a spectrum of gamma-rays with peaks corresponding to different energies. The area under each peak is proportional to the intensity of the corresponding gamma-ray, Figure 1.

Gamma-ray peaks of trace element are numbered as follows:

1 - Sm ¹⁵³	11 - Ta ¹⁸²	21 - Sr ⁸⁵
2 - U ²³⁹	12 - Nd ¹⁴⁷	22 - Cs ¹³⁴
3 - Yb ¹⁶⁹	13 - Eu ¹⁵²	23 - Rb ⁸⁶
4 - La ¹⁴⁰	14 - Ba ¹³¹	24 - Co ⁶⁰
5 - W ¹⁸⁷	15 - Hf ¹⁸¹	26 - Tb ¹⁶⁰
6 - As ⁷⁶	16 - Ce ¹⁴¹	
7 - Sb ¹²²	17 - Ca ⁴⁷	
8 - Sc ⁴⁸	18 - Lu ¹⁷⁷	
9 - Fe ⁵⁹	19 - Th ²³³	
10 - Na ²⁴	20 - Cr ⁵¹	

Figure 1. Gamma-ray spectra of sample [X-DR] obtained from activation measurements made five (Figure 1a) and seventeen (Figure 1b) days after irradiation, respectively

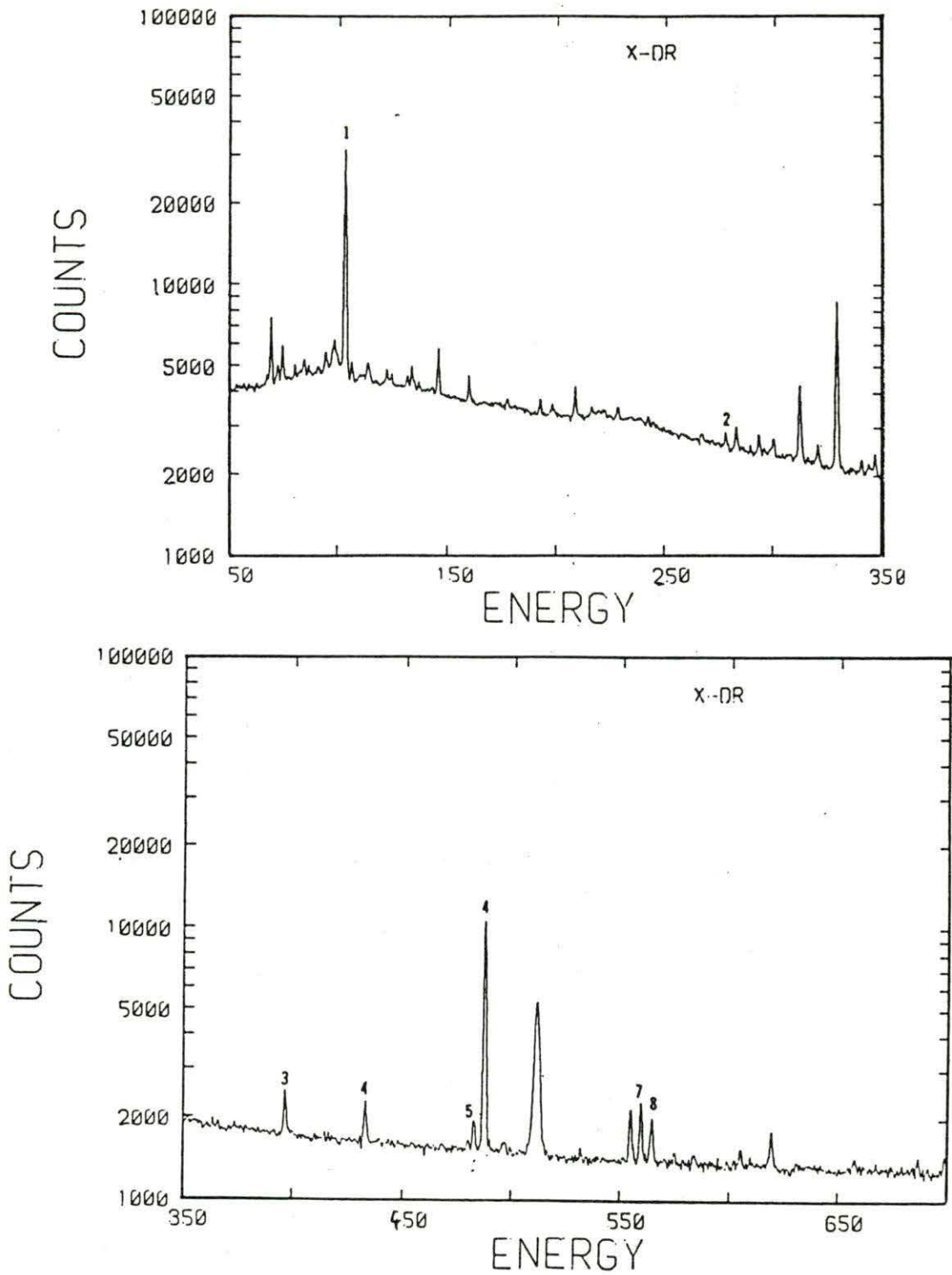


Figure 1a

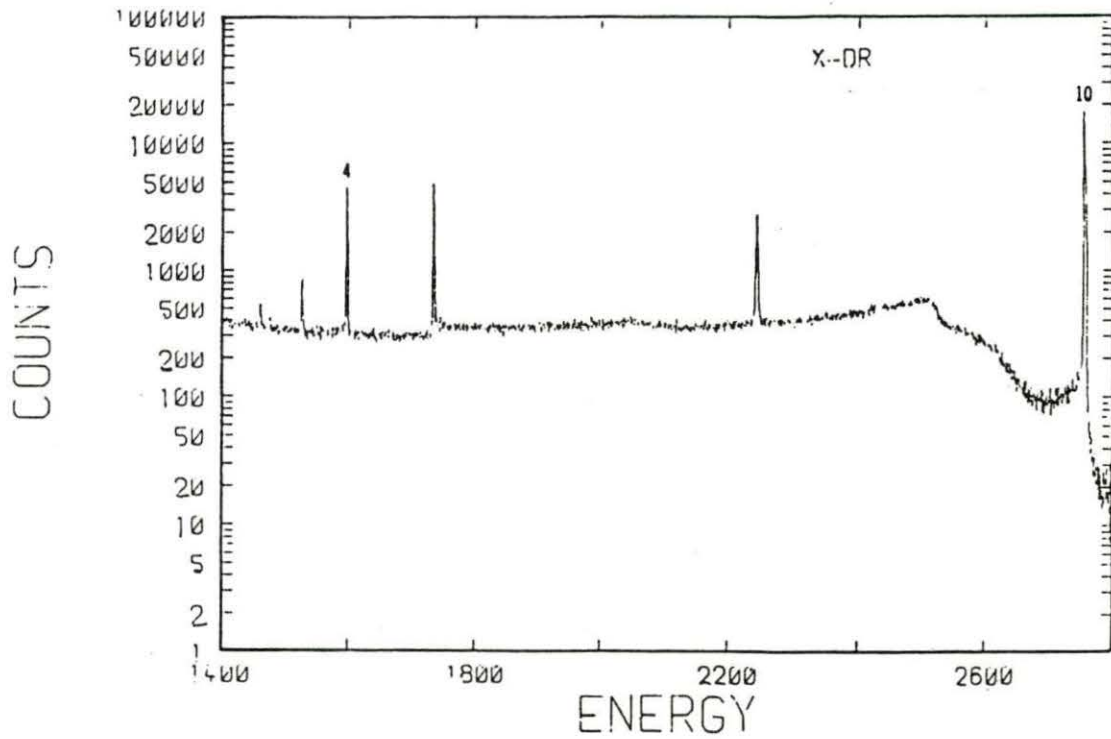
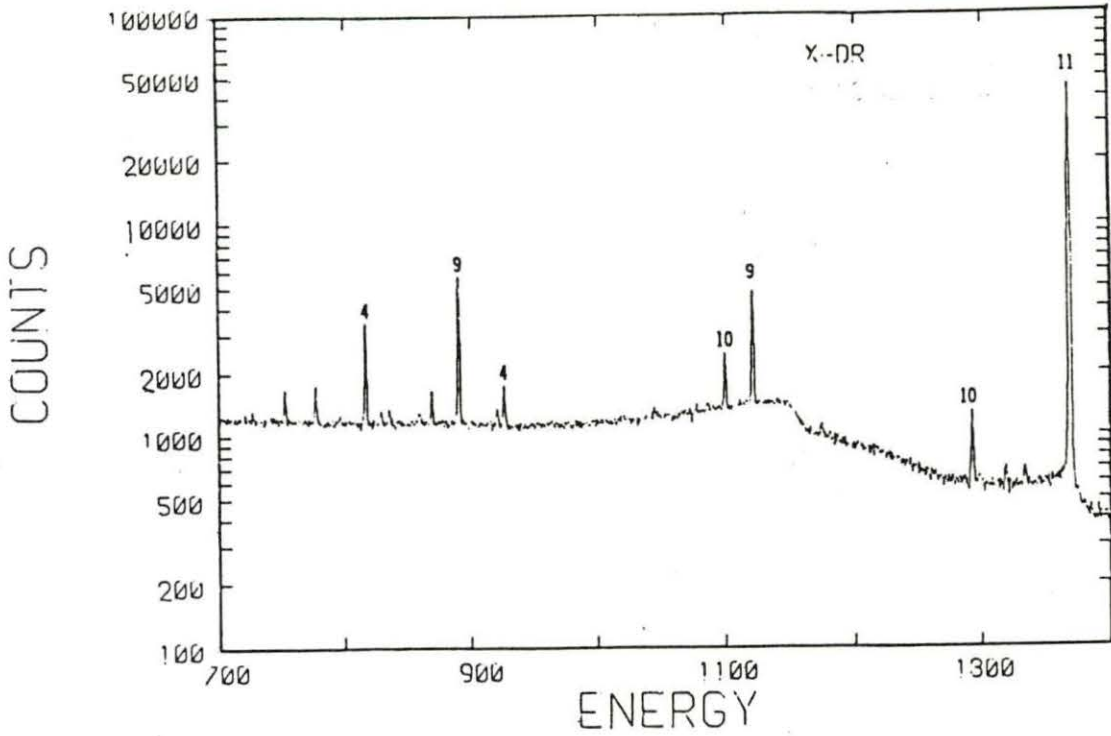


Figure 1a. continued

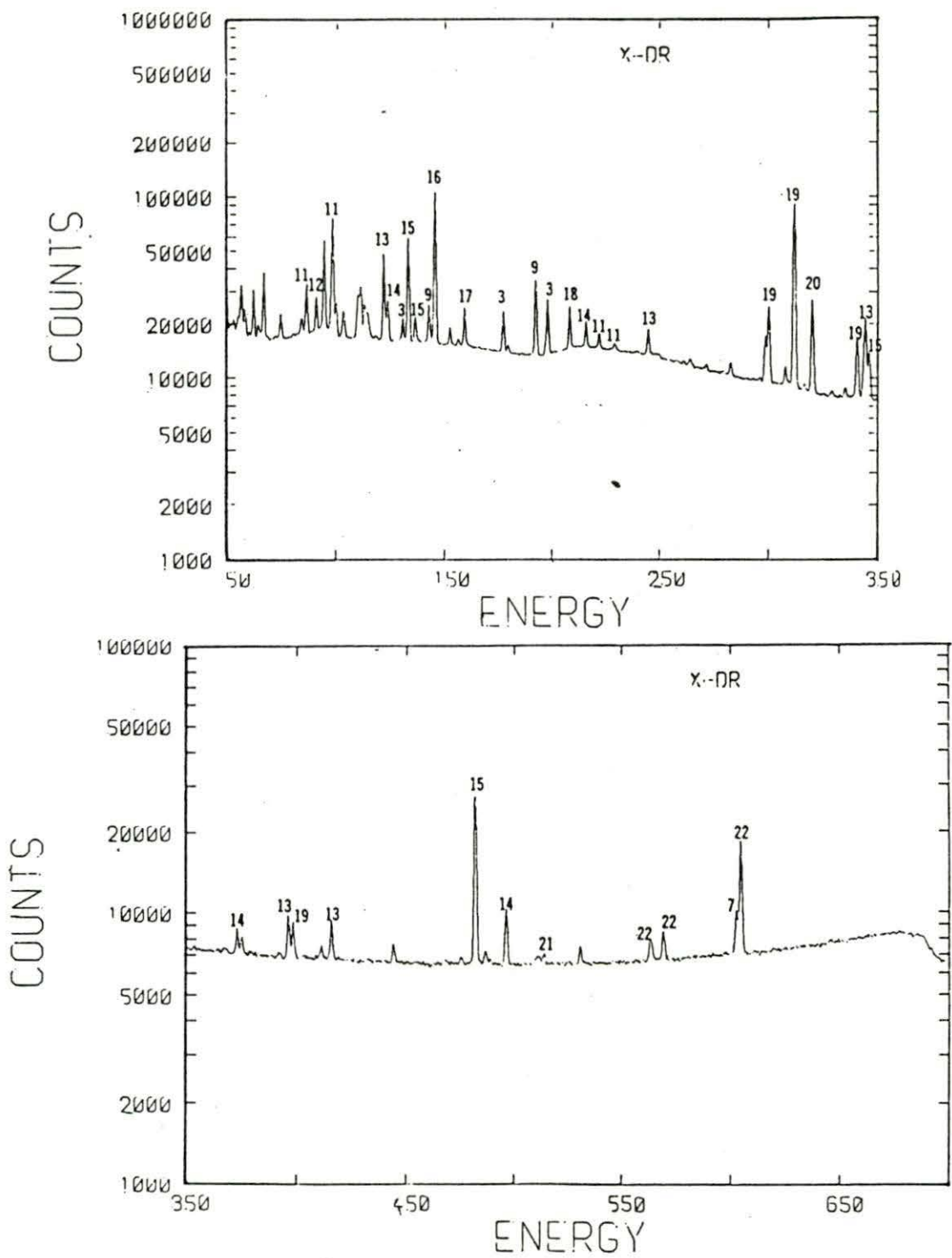


Figure 1b

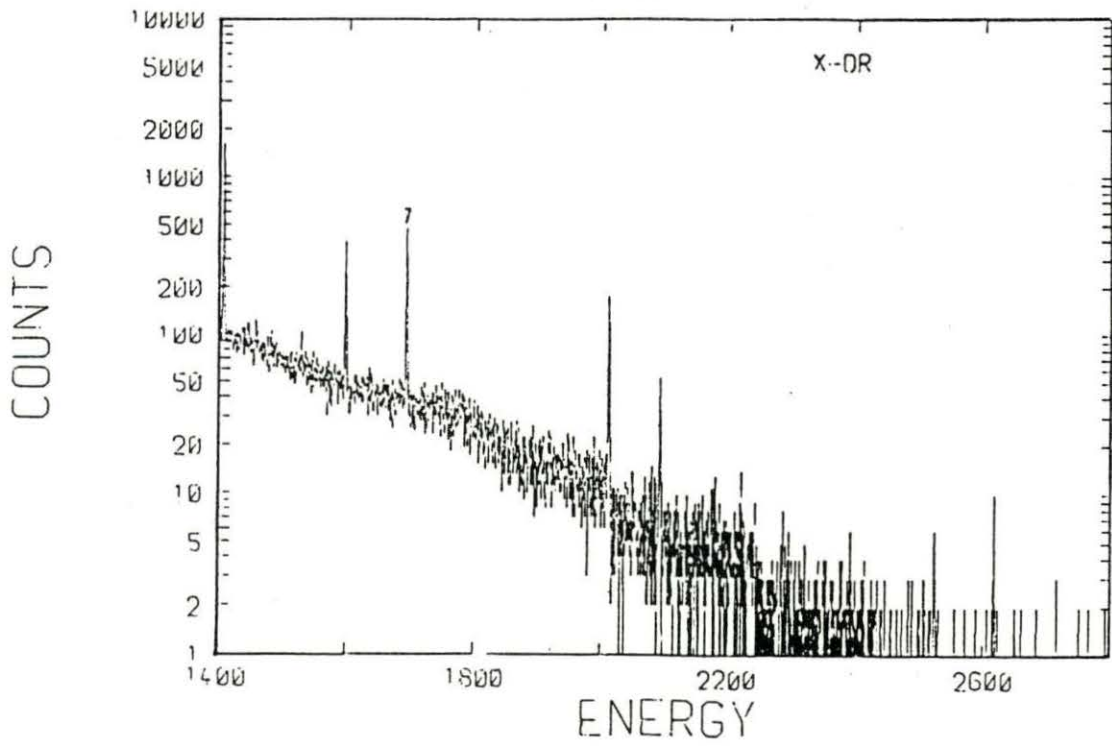
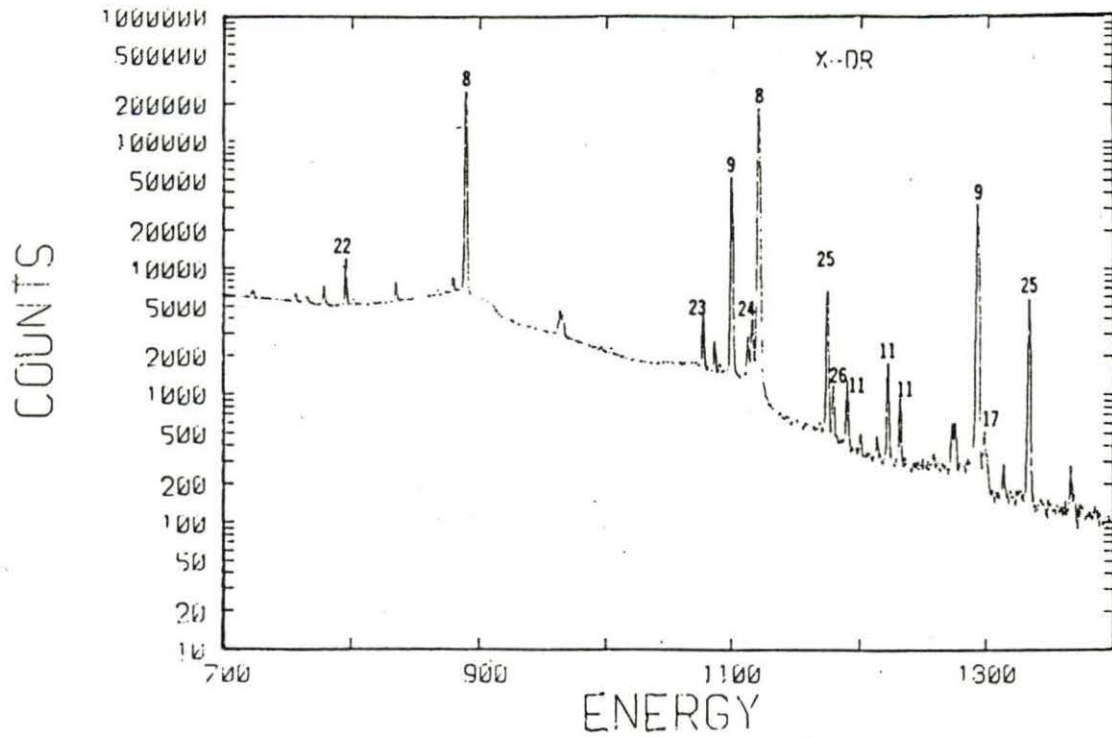


Figure 1b. continued

An absolute, or parametric, neutron activation determination, in which neutron-capture cross-sections, neutron flux, and the absolute sample activity must all be known with a high precision, is very difficult [20,26]. Instead, the standard, or comparator, technique, featuring a standard sample of known composition is widely used. In this technique, a standard sample and the unknown are irradiated simultaneously under the same conditions. If activity measurements are also made under the same identical conditions, (i.e., $t_{c_{uk}} = t_{c_{st}}$) all of the above-mentioned terms will not be involved in the calculations since they cancel in pairs. The ratio of the activities of the unknown sample to the standard sample is the same as the ratio of the corresponding concentration of each element analyzed.

$$\frac{A_{uk}}{A_{st}} = \frac{\phi \sigma N_{uk} (1 - e^{-\lambda t_{uk}})}{\phi \sigma N_{st} (1 - e^{-\lambda t_{st}})}$$

If the activity rate is corrected to saturation, i.e., $t_{uk} = t_{st}$, then

$$\frac{A_{uk}}{A_{st}} = \frac{N_{uk}}{N_{st}} = \frac{W_{uk} C_{uk}}{W_{st} C_{st}}$$

where W_{uk} and W_{st} are the weight of the unknown and standard samples (in grams), respectively, and C_{uk} and C_{st} are the concentrations of the unknown and standard in parts per million. If C_{st} and W_{st} are selected, and A_{uk} and A_{st} are measured, then C_{uk} can be calculated from the equation:

$$C_{uk} = \frac{A_{uk}/W_{uk}}{A_{st}/W_{st}} C_{st}$$

The comparator technique is used in this study.

The precision of the C_{uk} determination can be found using propagation of errors [36]:

$$C_{uk} \pm \Delta C_{uk} = C_{st} A_R \theta_R D_R \left[1 \pm \sqrt{\left(\frac{\Delta C_{st}}{C_{st}}\right)^2 + \left(\frac{\Delta A_R}{A_R}\right)^2 + \left(\frac{\Delta \theta_R}{\theta_R}\right)^2 + \left(\frac{\Delta D_R}{D_R}\right)^2} \right]$$

in which the full energy peak ratio

$$A_R \pm \Delta A_R = \frac{A_{uk}}{A_{st}} \left[1 \pm \sqrt{\left(\frac{\Delta A_{uk}}{A_{uk}}\right)^2 + \left(\frac{\Delta A_{st}}{A_{st}}\right)^2} \right]$$

the counting geometry ratio

$$\theta_R \pm \Delta \theta_R = \frac{\theta_{st}}{\theta_{uk}} \left[1 \pm \sqrt{\left(\frac{\Delta \theta_{st}}{\theta_{st}}\right)^2 + \left(\frac{\Delta \theta_{uk}}{\theta_{uk}}\right)^2} \right]$$

the decay ratio

$$D_R \pm \Delta D_R = \frac{e^{-\lambda t_{d_{st}}}}{e^{-\lambda t_{d_{uk}}}} \left[1 \pm \sqrt{(\lambda \Delta t_{d_{st}})^2 + (\tau_{d_{st}} \Delta \lambda)^2 + (\lambda \Delta t_{d_{uk}})^2 + (\tau_{d_{uk}} \Delta \lambda)^2} \right]$$

1.3. Studies of Mesoamerican Pottery

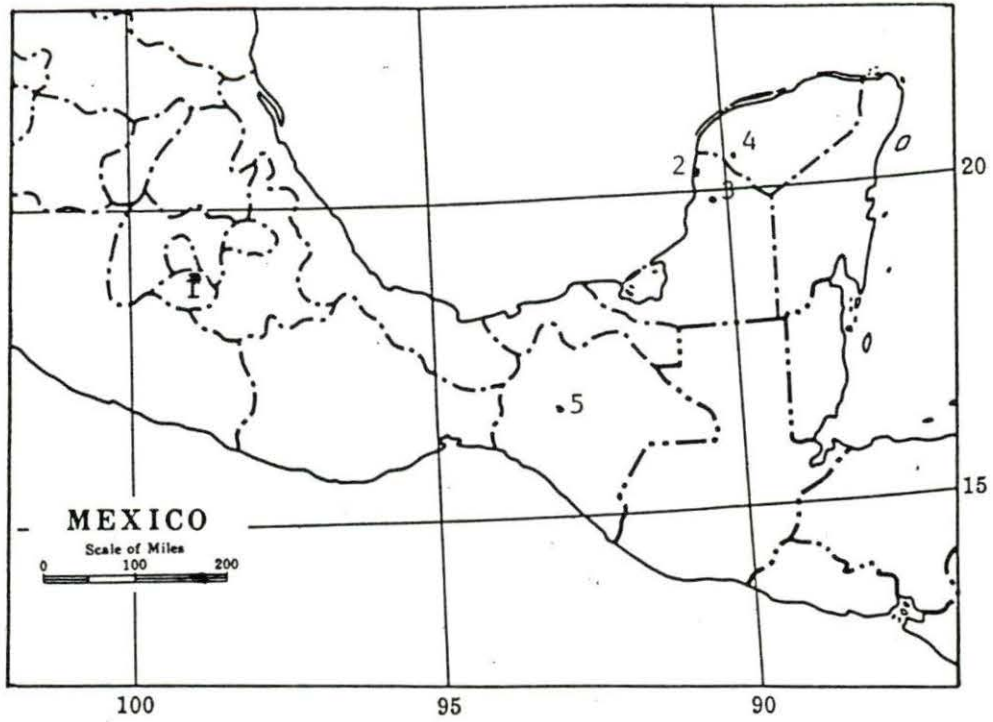
Ceramic products from different sites in Mesoamerica were among the first to be studied by neutron activation analysis. The major investigations were concerned with the Maya Fine Orange ware a relatively luxurious pottery found at many ceremonial centers of classic and post-classic Maya periods. In the late fifties, Sayer et al. [41] studied fragments of this pottery which came from two widely separated

sites (Kixpek in Southern Guatamalan highlands and Piedras Negras in central low lands [38]). Later in the seventies, Sayer, Chan, and Sabloff made a similar study on 45 Fine Orange fragments from nine Maya sites extending from southern Guatamalan high-lands to Chichen Itza in Yucatan, and from the Mexican province of Tabasco to British Honduras [42]. In both studies, the local utilitarian pottery was found not to match in composition the Fine Orange pottery. An independent intervening study [13] done on these pottery wares gave the same results.

Along with the Mayan Fine Orange ware, the Mexican classic-period potteries were also analyzed. Johnson et al. [22] and Bennyhoff et al. [7] studied pottery fragments from Cuicuilco and from Teotihuacan by determining the concentration of only one element, manganese. Another study [1] shed some light on the question raised by the presence of Oaxacan ceramic products at Teotihuacan. An obvious possibility is that trade took place between the two centers during early classic times.

1.4. Samples Description and Origin [Figure 2]

All the potshard samples, except one, used in this investigation were provided by the Anthropological Museum of Mexico (In Mexico City). And were provided by Mrs. Trini Martinez of the Department of Chemistry of the University of Mexico. The information currently available about the samples consists of a brief description and the identification of the places where the shards were found. The remaining sample was found in debris associated with the reconstruction of the Nunnery at Uxmal, Yucatan. This sample was made of fine clay and uncolored.



Key

- 1 = Santa Cruz Acalpíxca, Xachimilco
- 2 = Edzna, Campeche
- 3 = Jaina, Campeche
- 4 = Uxmal, Yucatan
- 5 = Chiapa de Corzo, Chiapas

Figure 2. Map illustrating location from which samples were excavated

1.4.1. Samples from Santa Cruz Acalpixca, Xachimilco

This collection consist of four potshards:

- i) Sample #7 is a shard from the upper part of a fine clay pot. The pot was decorated with black on an orange base.
- ii) Sample #8 is a shard from the upper part of a pot. It was glazed on the exterior and colored with black over red.
- iii) Sample #8b is a shard from the upper part of pot glazed on the interior and decorated with red band over the clay color.
- iv) Sample #9 is also a shard from an upper part of a pot glazed on the exterior with a black over red, while the interior was finished with a red glaze only.

1.4.2. Samples from Campeche

This collection consist of three samples from Edzna and one from Jaina, respectively:

- i) Sample #10 is polished with red-orange.
- ii) Sample #11 is decorated with yellowish cream.
- iii) Sample #12 is of fine grain type.
- iv) Sample #14 is decorated with a light red-coffee color.

1.4.3. Samples from Chiapa de Corzo, Chiapas

This group consists of two samples:

- i) Sample #13 is of liberated type, decorated with black-coffee color.
- ii) Sample #19 is from Tapalapa cerro hueco group.

The information given above is all that is available at this time. It is hoped that more information can be found to assist with the interpretation of the experimental findings such as the relations between these respective populations centers. Thus, this work will be limited to a study of the compositional similarities or dissimilarities among the samples described above.

2. EXPERIMENTAL PROCEDURE

The analytical procedures employed in this study were adapted from experimental works by Perlman and Asaro [33], Bieber et al. [8], and Brooks et al. [11], and apply to techniques used in the Research Reactor Facility at the University of Missouri.

2.1. Sampling, Encapsulation, and Irradiation

The pottery shard sampling was done at the Research Reactor Facility at the University of Missouri, MURR. First, the potshards were scraped by a hand-held synthetic sapphire rod (1 mm diameter), to remove the potentially contaminated outer surface area in preparation for actual sampling. Then potshards were scraped again to obtain 300 mg of sample in powdered form. This powder was collected on a clean index card, from which it was poured into a clean polyethylene sample vial with a snap top (The MURR facility provides specially cleaned receptacles for activation analysis purposes).

High purity quartz vials (T-21) were labeled, by scratching reference numbers on each. Although a pottery powder sample weight of 50 mg was intended, the weight of the actual samples varied from 35-120 mg. Except samples for 7, 8b, and 9, three replicas of each sample were provided. The tubes containing the powder were then heat-sealed, wrapped in aluminum foil to form bundles, and put in an aluminum can for irradiation. The samples were irradiated in the MURR reactor for 24 hours at a flux of 5×10^{13} neutrons per square centimeter per second.

2.2. Standardization

Six United States Geological Survey analyzed "standard" rocks were used as standards in the study done by Bieber et al. [8]; however, space limitations in the aluminum irradiation can required that this procedure be replaced. Three replicates of fly ash (NBS-1633A) were used as standards in this work. The composition of fly ash as a standard has been established [20], and can, in this case, serve as a good substitute for the six USGS standards.

The three standard replicates were packed with the samples in the same aluminum can, so that the calculation of trace element concentrations in the samples is simplified. This composition method makes it possible to eliminate the following from the calculation: the irradiation time, neutron flux, ratio of thermal to fast and epithermal neutrons, the neutron-capture cross-sections and the necessity of knowing the absolute gamma-ray intensity along with the detector efficiency for each radioactive element formed.

2.3. Gamma Ray Detection

All of the gamma-ray detection and pulse-height analysis was done using equipment provided by the Research Reactor Facility, University of Missouri, MURR. About five days after irradiation, standards and samples were gamma counted using a sample changer detector system. The time for activity measurement was 1800 seconds. Seventeen days later, activity measurements were taken again but for 7200 seconds.

The sample changer detector system used consisted of the following: Nuclear Chicago sample changer, which had been modified by MURR for use

with Ge (Li) detectors. Judiciously placed lead shielding (approximately 8 inches) prevents radiation from samples waiting to be counted from reaching the detector while it is counting photons from the current sample. The radiation detector was a Princeton Gamma Tech lithium-drifted germanium detector (serial number 2419). Its efficiency relative to a 3 x 3 NaI detector was about 17%. The resolution is about 1.8 KeV for the 1332 KeV gamma-ray from Co^{60} . The pulses were fed from the detector to a preamplifier, then to an amplifier (ORTEC 572) and to a Nuclear Data (ND 570) 8192 channel pulse height analyzer. The dead time was kept to about 10% to minimize pulse-pile-up error. The appropriate corrections were made at the time of analysis. The output of the ND 570 analyzer was placed in the memory of a Nuclear Data 6620 analyzer system, which controls counting, sample changing, and storage of data onto a Winchester disk drive and a magnetic tape. The connection of sample changer detector system is presented in Figure 3, while a typical spectra obtained from the first and second activity measurements are shown in Figures 1a and 1b, respectively.

2.4. Spectrum Analysis and Determination of Trace-Element Concentrations

The magnetic tape, containing the experimented data, was read and analyzed using the following computer programs: NAPARS, HEAD, TPRINT, PEAK, NSTD, STDPRT, CRITIC, NUNK, NAAOUT, and OUTPUT (see Figure 4).

The first program, NAPARS is an input program that reads the reference table of isotopes and gamma-ray energies to be used for identification; it also reads relevant data relating to the standards

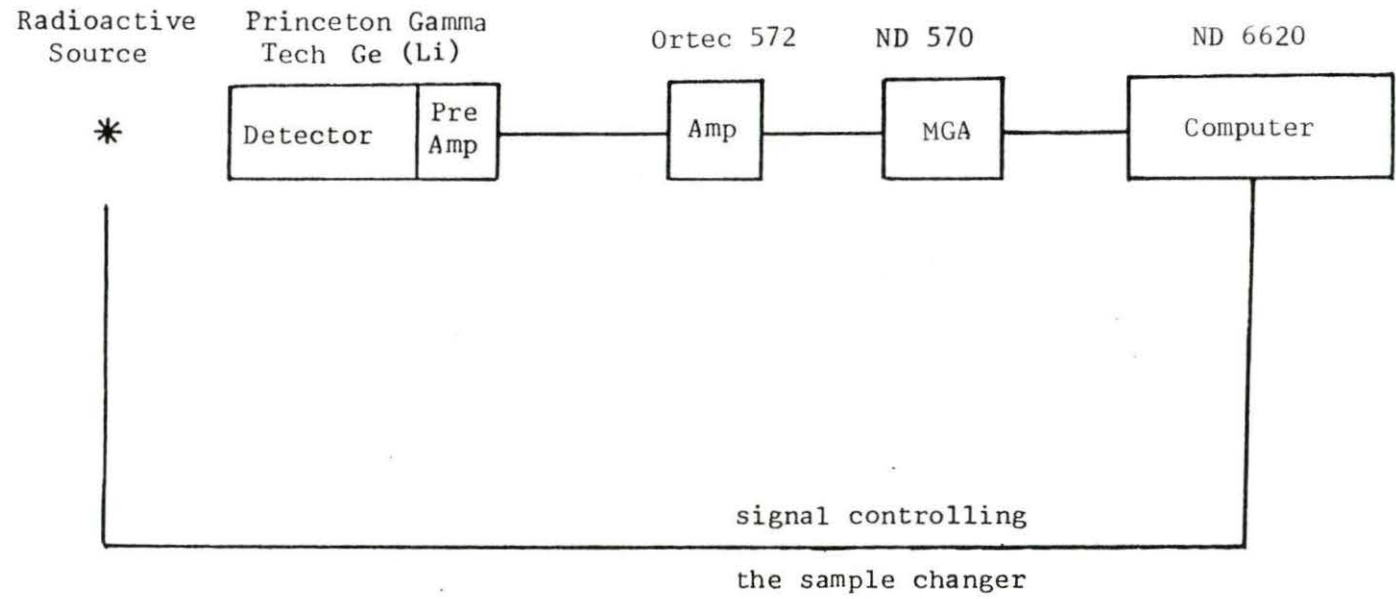


Figure 3. Sample changer detector system connection

including the concentration of each element in them. The second program, HEAD, is another input program which reads the data pertaining to the samples including identification, weight, count duration, energy channel calibration information, peak search and fitting parameters, and reference data. The third program, TPRINT, calculate the ADC dead time and the decay time for a particular sample. The fourth program, PEAK, scans the spectrum (typical spectra are shown in Figure 1) to locate all the significant peaks and then calculates the net area of each peak. Energies are assigned to the peaks using a straight line equation stored in program HEAD. The fifth program, NSTD, gives a summary of peaks identified in program PEAK and calculates a constant for each peak. This constant is

$$\text{Constant} = \frac{\text{Cou}_{st}}{W_{st}} C_{st} e^{+\lambda t_d}$$

where:

Cou_{st} = number of counts per sec for the element in the standard

W_{st} = standard sample weight (mg)

C_{st} = concentration of the element in standard

= decay constant = $\frac{\ln 2}{T_{1/2}}$

$T_{1/2}$ = half-life for the isotope

t_d = time between end of irradiation and midpoint of count

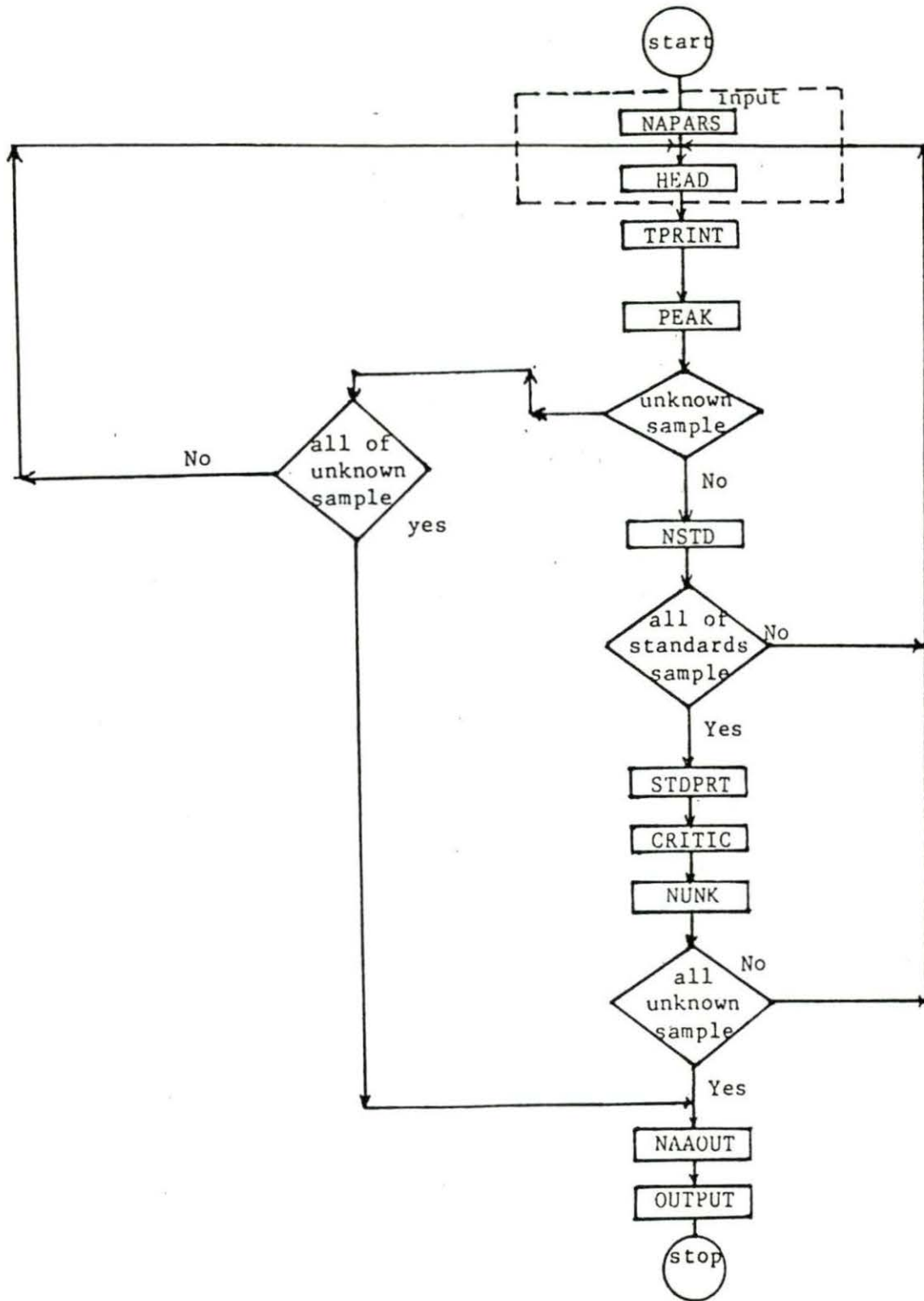


Figure 4. Spectrum analysis and trace element determination flowchart

The second, third, fourth, and fifth programs were repeated for each of the standard replicates. The sixth program, STDPRT, lists a summary of the constant for each element. Then the seventh program, CRITIC, evaluates the constant from the replicates of the standards to reject inconsistent values, and finally calculates the mean value of each constant.

As shown in the flow chart (Figure 4), HEAD, TPRINT, and PEAK programs were used to measure count rates and the areas under the curves corresponding to different elements in the unknown samples. Using this output and the mean values of the standards' constants calculated by CRITIC, the eighth program, NUNK, computes the concentration of each element in the unknown samples as follows:

$$C_{uk} = [Cou_{uk}/W_{uk}] \frac{e^{-t_d}}{\text{constant}}$$

where C_{uk} = concentration of the element in the unknown sample

Cou_{uk} = the count rate (number/sec) for the element in the unknown sample

W_{uk} = the unknown sample weight in mgs.

A summary of the concentrations of every element in every replicate of the unknown sample is provided by the ninth program, NAAOUT.

The last program, OUTPUT, evaluates the concentrations of each element in the three replicates of the unknown sample and rejects any inconsistent value. Then it calculates the averages and the standard deviation for each case. Therefore the final result is a list that contains the unweighted mean of the concentration, the unweighted

standard deviation of the sample, the standard deviation of the sample, the weighted mean of concentrations, and the weighted standard deviation of the sample. A list of the elements composing the standard sample are given in Table 1, while the list of elements determined in the unknown samples are shown in Table 2.

2.5. Discussion of Experimental Procedure

In principle, the significance of the analysis improves a) as the number of elements involved in the determination increases and b) with the precision with which the elements are determined. Of course, if one particular element is present at a concentration level that cannot be determined with sufficient accuracy, compromising between these two factors is necessary.

Neutron activation analysis technique is in many cases so sensitive that many elements can be determined down to trace levels (parts per million). Certain elements cannot be determined by this method because they have either very small neutron activation cross sections or very short half-lives and thus decay before measurement of activity can be made. Some of these element are of possibly great value in characterizing clays. Lead is the most important one. However some other elements, e.g., oxygen, hydrogen, silicon, carbon, and aluminum are major constituents of most clays and pottery. Thus it is a significant advantage that they cannot be determined by neutron activation analysis, and so will not interfere with the determination of trace elements.

Table 1. Element concentration in NBS-1633a fly ash [20]

Element	Units	Consensus Value	
B	(ppm)	39.2	+ 1.0
Na	(%)	0.165	+ 0.004
Mg	(%)	0.455	+ 0.010
Al	(%)	14.0	+ 1.0
Si	(%)	22.8	+ 0.8
S	(%)	0.27	+ 0.01
Cl	(ppm)		---
K	(%)	1.88	+ 0.08
Ca	(%)	1.11	+ 0.01
Sc	(ppm)	38.6	+ 1.1
Ti	(%)	0.80	+ 0.1
V	(ppm)	300.	+ 50.
Cr	(ppm)	193.	+ 5.
Mn	(ppm)	190.	+ 10.
Fe	(%)	9.51	+ 0.18
Co	(ppm)	44.1	+ 1.0
Ni	(ppm)	130.	+ 27.
Zn	(ppm)	220.	+ 10.
Ga	(ppm)	58.	+ 5.
As	(ppm)	145.	+ 3.
Se	(ppm)	10.3	+ 0.6
Br	(ppm)	2.31	+ 0.16
Rb	(ppm)	134.	+ 4.
Sr	(ppm)	835.	+ 40.
Zr	(ppm)	240.	+ 30.
Mo	(ppm)	31.3	+ 3.6
Ag	(ppm)		---
Cd	(ppm)	1.0	+ 0.2
Sb	(ppm)	6.15	+ 0.15
Cs	(ppm)	10.4	+ 0.2
Ba	(ppm)	1320.	+ 40.
La	(ppm)	76.7	+ 0.4
Ce	(ppm)	168.8	+ 1.2
Nd	(ppm)	81.4	+ 2.5
Sm	(ppm)	16.6	+ 0.13

Table 1. continued

Element	Units	Consensus Value
Eu	(ppm)	3.50 + 0.04
Gd	(ppm)	16.0 + 0.2
Tb	(ppm)	2.69 + 0.07
Dy	(ppm)	---
Yb	(ppm)	7.68 + 0.09
Lu	(ppm)	1.146 + 0.020
Hf	(ppm)	7.29 + 0.22
Ta	(ppm)	1.93 + 0.07
W	(ppm)	4.6 + 0.5
Ir	(ppb)	---
Au	(ppb)	---
Th	(ppm)	24.0 + 0.3
U	(ppm)	10.3 + 0.3

Table 2. Element concentration in the unknown samples (concentration in parts per million except for Na and Fe which are in % x 10⁴)

Samples	7	8	8b	9	10	11
Elements						
Na-24	11139 +209	10764.5 +325.185	9342 +176.0	9982 190.	7776.46 +137.59	8694.63 +165.
As-76	3.105 +.584	3.1772 +.2072	6.916 +.798	- -	8.28977 +.4535	13.1619 +1.274
Sb-122	.8207 +.1378	- -	- -	- -	2.93342 +.1804	1.61004 +.2126
La-140	24.89 +.37	28.4098 +.8375	27.02 +.46	23.27 +.63	29.7737 +.3491	27.8228 +.4574
Sm-153	5.572 +.296	6.60024 +.2581	7.015 +.369	4.826 +.498	7.98278 +.5677	4.80062 +.6405
Yb-175	2.372 +.384	2.68064 +.3941	2.98 +.484	2.932 +.726	4603 +.765	3.06716 +.2715
U(Np-239)	- -	2.9006 +.8513	- -	- -	2.62631 +.568	3.35799 +.703
Sc-46	14.47 +.24	16.3667 +.3909	14.81 +.25	13.01 +.22	9.99008 +.1657	8.47699 +.141
Cr-51	106.0 +1.8	114.644 +2.8992	100.4 +1.8	77.18 +1.52	26.7949 +.5677	55.0264 +1.0548
Fe-59	4,2913 +483	46861.4 +207.17	43769 +498	37987 +442	20756 +236.937	22318.2 +260.168
Co-60	18.59 +.26	17.5138 +.4251	16.37 +.24	15.42 +.24	8.08964 +.1201	6.25691 +.1076
Zn-65	84.89 +2.96	85.9076 +2.5215	88.53 +3.25	77.18 +3.23	56.1459 +1.9431	72.3119 +6.093
Rb-86	52.78 +2.37	86.0795 +4.8457	79.06 +3.4	60.46 +3.54	156.706 +11.6773	74.1123 +2.9688
Sr-85	415 +35.8	522.129 +15.4319	541.9 +46.1	246.7 +42.6	166.34 +18.6166	108.303 +23.5558

Samples	12	13	14	19	DR	Average of Group C
Elements						
Na-24	13696.4 <u>+143.688</u>	7241.32 <u>+138.322</u>	2176.97 <u>+61.101</u>	6619.43 <u>+238.581</u>	6461.71 <u>+121.761</u>	10306875 <u>+803.8</u>
As-76	21.5224 <u>+.42</u>	14.3728 <u>+.7958</u>	13.3576 <u>+1.0591</u>	3.90638 <u>+.0641</u>	10.5085 <u>+.2833</u>	3.118 <u>+2.5</u>
Sb-122	- -	.970859 <u>+.4016</u>	2.44297 <u>+.0754</u>	- -	1.69874 <u>+.0916</u>	- -
La-140	16.0348 <u>+.03195</u>	25.1202 <u>+.4784</u>	14.395 <u>+.3994</u>	18.3523 <u>+.2287</u>	31.8975 <u>+.3454</u>	25.89 <u>+2.27</u>
Sm-153	4.70966 <u>+.4006</u>	6.15488 <u>+.1428</u>	3.35643 <u>+.0423</u>	4.27691 <u>+.1178</u>	5.22599 <u>+.1135</u>	6.003 <u>+.99</u>
Yb-175	1.51813 <u>+.2106</u>	3.56157 <u>+.3648</u>	3.26355 <u>+.4541</u>	2.06121 <u>+.2718</u>	3.71893 <u>+.3078</u>	2.74 <u>+.28</u>
U(Np-239)	- -	3.18404 <u>+.4183</u>	4.03873 <u>+.7385</u>	- -	2.539358 <u>+.2721</u>	- -
Sc-46	10.7693 <u>.0066</u>	9.87953 <u>+.1643</u>	14.9034 <u>+.247</u>	8.66495 <u>+.1866</u>	11.074 <u>+.1836</u>	14.66 <u>+1.4</u>
Cr-51	86.2018 <u>+.613</u>	202.149 <u>+3.308</u>	100.035 <u>+3.35</u>	17.2759 <u>+1.0556</u>	59.7072 <u>+.2409</u>	99.61 <u>+16</u>
Fe-59	32952.4 <u>+202.513</u>	41165.5 <u>+470.64</u>	35660.7 <u>+404.175</u>	26261.1 <u>+555.387</u>	32230.8 <u>+367.82</u>	42882.6 <u>+3678.06</u>
Co-60	12.8756 <u>+.1856</u>	13.8302 <u>+.2089</u>	8.29063 <u>+.1272</u>	4.79513 <u>+.1132</u>	8.21374 <u>+.0792</u>	16.97 <u>+1.4</u>
Zn-65	65.51 <u>+.8464</u>	82.6743 <u>+3.0401</u>	84.0632 <u>+3.9942</u>	60.0523 <u>+2.9554</u>	78.9935 <u>+5.105</u>	84.13 <u>+4.9</u>
Rb-86	42.0934 <u>+2.451</u>	54.9355 <u>+2.9576</u>	28.3106 <u>+1.2147</u>	44.7872 <u>+2.0957</u>	86.7028 <u>+6.0848</u>	69.58 <u>+15.6</u>
Sr-85	733.106 <u>+38.1883</u>	463.162 <u>+16.6334</u>	102.049 <u>+76.179</u>	361.986 <u>+60.7019</u>	104.03 <u>+30.0459</u>	431.43 <u>+135.2</u>

Samples	7	8	8b	9	10	11
Elements						
Sb-124	.3783 ±.041	.411817 ±.0549	.4475 ±.0458	.4657 ±.0564	2.19907 ±1.0673	1.7393 ±1.0558
Cs-134	3.889 ±.121	4.14799 ±.0759	3.658 ±.128	3.232 ±.131	15.3569 ±.8295	4.43856 ±.1278
Ce-141	52.48 ±.36	57.4471 ±.4286	52.9 ±.42	51.34 ±.49	58.9827 ±.3627	45.6547 ±.3575
Nd-147	28.2 ±1.06	33.7849 ±1.3169	34.29 ±1.37	26.27 ±1.38	38.6877 ±1.2455	20.9468 ±2.3492
Eu-152	1.565 ±.024	1.66051 ±.0553	1.636 ±.028	1.48 ±.031	1.13779 ±.01889	.664501 ±.016
Tb-160	.8319 ±.057	.979488 ±.0949	.9449 ±.0686	.8076 ±.0764	1.56148 ±.0148	.833847 ±.0595
Yb-169	2.007 ±.052	2.39864 ±.0621	- -	2.258 ±.078	4.13566 ±.0699	2.07588 ±.0491
Hf-181	5.782 ±.133	6.30624 ±.241	6.178 ±.144	5.479 ±.145	6.29312 ±.1382	5.11058 ±.1207
Ta-182	.6308 ±.0331	.765885 ±.0064	.6824 ±.0377	.6121 ±.0420	1.49666 ±0.531	1.33586 ±.0808
Th(Pa-233)	5.47 ±.062	6.13469 ±.11176	6.024 ±.075	6.03 ±.088	11.7424 ±.1031	13.2456 ±1.204
Lu-177	.321 ±.0121	.34979 ±.0206	.3513 ±.0138	.3352 ±.0171	.458022 ±.0126	.3219 ±.0136

• Samples • • • Elements •	12	13	14	19	DR	Average of Group C
Sb-124	.296789 ±.06156	.629793 ±.1006	2.6875 ±.0819	.24972 ±.0459	1.83386 ±.12626	.4258 ±.039
Cs-134	1.34016 ±.0053	2.96104 ±.1103	3.90805 ±.593	1.27613 ±.0823	5.67733 ±.2965	3.73 ±.39
Ce-141	33.4432 ±.4771	54.5167 ±.4281	96.2027 ±.5703	44.4753 ±.3516	88.9805 ±.5446	53.54 ±2.9
Nd-147	18.8066 ±.0653	23.7647 ±1.2422	13.2703 ±1.497	22.1085 ±1.3343	29.4776 ±2.006	30.64 ±4.01
Eu-152	1.20986 ±.0186	1.4703 ±.0293	.732071 ±0.247	1.34585 ±.0414	.962169 ±.0161	1.585 ±.081
Tb-160	.48354 ±.0036	.938319 ±.008	.757167 ±.0433	.645086 ±.0635	.818681 ±.0716	.891 ±.08403
Yb-169	1.27684 ±.0217	2.88775 ±.1514	2.80373 ±.063	1.57855 ±.0329	3.28006 ±.1414	2.22 ±.1975
Hf-181	3.74087 ±.1633	4.81921 ±.0855	7.49798 ±.1673	5.82346 ±.1865	7.04838 ±.3753	5.924 ±.37
Ta-182	.343123 ±.0106	.919756 ±.0293	1.31891 ±.1007	.460534 ±.0525	1.36609 ±.0681	.673 ±.0688
Th(Pa-233)	2.98847 ±.0284	7.86869 ±.0872	18.0515 ±.1566	4.391 ±.0024	17.4737 ±.147	5.91 ±.3
Lu-177	.188487 ±.0080	.326958 ±.015	.491115 ±.0074	.245034 ±.0779	.52941 ±.01417	.339 ±.014

In principle, activation analysis can involve isotopes with any measurable half-life from the very short to the very long. In many cases it is both convenient and adequate to consider only those isotopes with intermediate to long half-lives.

Elements with half-lives between one hour and one week suitable for neutron activation analysis include those given in Table 3a. Of these elements molybdenum and calcium were not determined in this analysis.

In order to minimize the statistical error, the element concentration measurements of a peak were taken within 8 half-lives from the end of the irradiation. Despite this precaution, some results were unacceptably large. Tungsten, W-187, was measured in three samples and standard deviations of 40%, 30%, and 38% were found. Thus the contribution of tungsten to the comparison was ignored in the final analysis. Ni(Co58) was detected in five samples with 48%, 48.45%, 45%, 71.67%, and 17% standard deviations, and this contribution too was ignored.

The use of Fly Ash standard in this study prevented the determination of some elements which were determined by others in other studies. Among these were manganese and potassium. The element calcium is weakly activated by neutron flux. However, it occurs in some ceramics as a major constituent, in which case its presence will be determined. Unfortunately, the program PEAK did not detect calcium in any of the three replicates of the Fly Ash standard.

Table 3a. Gamma counted elements five days after irradiation

Element	Energy (KeV)	Half-Life	Sec
Na-24	1368.60	0.5000E 01 H	5.4000E 04
Na-24	2754.00	1.5000E 01 H	5.4000E 04
Ca-47	1297.10	4.5400E 00 D	3.9226E 05
As-76	559.10	2.6300E 01 H	9.4680E 04
Br-82	554.30	3.5340E 01 H	1.2722E 05
Br-82	619.10	3.5340E 01 H	1.2722E 05
Br-82	776.50	3.5340E 01 H	1.2722E 05
Mo-99	140.40	6.6020E 01 H	2.3767E 05
Mo-99	181.10	6.6020E 01 H	2.3767E 05
Sb-122	564.10	2.6899E 00 D	2.3155E 05
Sb-122	692.80	2.6800E 00 D	2.3155E 05
La-140	328.80	4.0270E 00 H	1.4497E 05
La-140	487.00	4.0220E 01 H	1.4497E 05
La-140	815.80	4.0270E 01 H	1.4497E 05
La-140	1596.50	4.0270E 01 H	1.4497E 05
Sm-153	69.70	4.6800E 01 H	1.6848E 05
Sm-153	103.20	4.6800E 01 H	1.6848E 05
Yb-175	282.50	4.1900E 00 D	3.6202E 05
Yb-175	396.30	4.1900E 00 D	3.6202E 05
W-187	134.20	2.3900E 01 H	8.6040E 04
W-187	479.60	2.3900E 01 H	8.6040E 04
W-187	685.90	2.3900E 01 H	8.6040E 04
U(Np-239)	106.10	2.3500E 00 D	2.0304E 05
U(Np-239)	228.20	2.3500E 00 D	2.0304E 05
U(Np-239)	277.60	2.3500E 00 D	2.0304E 05

Table 3b. Gamma counted elements twenty one days after irradiation

Element	Energy (KeV)	Half-life	Sec
Sc-46	889.30	8.3800E 01 D	7.2403E 06
Sc-46	1120.50	8.3800E 01 D	7.2403E 06
Cr-51	320.10	2.7710E 01 D	2.3941E 06
Ff-59	1099.20	4.4600E 01 D	3.8534E 06
Ff-59	1291.60	4.4600E 01 D	3.8534E 06
Co-60	1173.20	5.2700E 00 Y	1.6619E 08
Co-60	1332.50	5.2700E 00 Y	1.6619E 08
Nt(Co-58)	810.80	7.0800E 01 D	6.1171E 06
Zn-65	1115.50	2.4370E 02 D	2.1056E 07
Se-75	279.50	1.2000E 02 D	1.0368E 07
Se-75	400.70	1.2000E 02 D	1.0368E 07
Rb-86	1076.60	1.8800E 01 D	1.6243E 06
Sr-85	514.00	6.4840E 01 D	5.6033E 06
Sb-124	602.70	6.0200E 01 D	5.2013E 06
Sb-124	722.80	6.0200E 01 D	5.2013E 06
Sb-124	1691.00	6.0200E 01 D	5.2013E 06
Cs-134	604.70	2.0600E 00 Y	6.4964E 07
Cs-134	795.80	2.0600E 00 Y	6.4964E 07
Ba-131	216.00	1.2000E 01 D	1.0368E 06
Ba-131	373.20	1.2000E 01 D	1.0368E 06
Ba-131	496.20	1.2000E 01 D	1.0368E 06
Ce-141	145.40	3.2500E 01 D	2.8080E 06
Nd-147	91.10	1.1000E 01 D	9.5040E 05
Nd-147	531.00	1.1000E 01 D	9.5040E 05
Eu-152	1408.00	1.3330E 01 Y	4.2037E 08
Eu-154	1274.80	8.8000E 00 Y	2.7752E 08
Tb-160	879.40	7.2100E 01 D	6.2294E 06
Tb-160	966.20	7.2100E 01 D	6.2294E 06
Tb-160	1178.00	7.2100E 01 D	6.2294E 06
Yb-169	177.20	3.2000E 01 D	2.7648E 06
Yb-169	197.90	3.2000E 01 D	2.7648E 06
Hf-181	346.00	4.2400E 01 D	3.6634E 06
Hf-181	482.20	4.2400E 01 D	3.6634E 06
Ta-182	1189.00	1.1500E 02 D	9.9360E 06
Ta-182	1221.40	1.1500E 02 D	9.9360E 06
Th(Pa-233)	300.10	2.7400E 02 D	2.3674E 06
Th(Pa-233)	312.00	2.7400E 01 D	2.3674E 06
Lu-177	112.90	6.7100E 00 D	5.7974E 05
Lu-177	208.40	6.7100E 00 D	5.7974E 05
Lu-177M	378.50	1.6000E 02 D	1.3824E 07

The ideal way to estimate the precision of an analytical method is to analyze the same pottery sample many times during the analysis program, then, for each element determined, to calculate the standard deviations of the concentration values. The variation in values can then be observed. Of course, space limitations within the irradiation can and sample size limitations precluded using this procedure. To eliminate a portion of the variation, the irradiation can was rotated to provide uniformity in the dose received by the samples and standards.

The uncertainty is reported with the element concentration in Table 2. The elemental concentrations obviously depend on the composition of the Fly Ash standard. Thus the overall uncertainty in the elemental concentrations will depend on two activation analysis determinations and the uncertainty associated with the Fly Ash standard elemental compositions. The values of the uncertainty presented in Table 2 are the ones to be used in case of internal comparisons among various samples analyzed in this study (i.e., the same standards are used in each case) while for a comparison with pottery analyzed using other standards, the uncertainty of the elements composing the Fly Ash must be taken into account along with those given in Table 2.

Possible errors have various sources: the weighing of the pottery powder contained in the quartz tubes and irradiation self-shielding within the can causing the standards and the sample to receive different neutron doses. Another two sources that contribute to the total uncertainty are the variations in the position of sample quartz tubes during the measurement of activity and the statistical uncertainty due to the statistical nature of radioactive decay.

3. RESULTS AND DISCUSSION

3.1. Theory of Grouping Procedures

The ultimate goal of the effort expended to obtain the data listed in Table 2, was to provide information of interest from an archeological point of view. This simply means that the presence or lack of differences between the concentrations of trace elements in different samples refute or support a common origin (location and technique) of those samples. Similarity analysis by the use of computerized data processing was preferred because the results are reproducible and they are quickly obtained. In this study, cluster analysis was used to form groupings and this was followed by visual inspection of the concentration curves in order to refine or confirm these groups.

3.1.1. Cluster Analysis

Most of the early works on classification and clustering were in the fields of zoology and biology, where it is generally known as taxonomy. Zubin and Thorndike were among those who started to use numerical classification techniques in fields other than natural science [18]. Then the technique spread in the sixties when computers became available to solve problems with large amount of computation. This classification technique was applied by Bieber et al. [8] and Beeck et al. [6] in the similarity analysis of pottery and is used in this investigation.

If information about a number of variables (element concentration) in an observation (a collection of element concentrations associated with a given shard or sample) is provided, then cluster analysis arranges similar observation into groups. This final grouping or classification

of the observation, usually allows the drawing of useful conclusions concerning the relationships among them.

The similarity or "closeness" between two observation (samples) is a measure of what they have in common. Furthermore, two observations are said to be "relatively similar" when they are close to each other in some way. Therefore, in order to treat this concept mathematically, "similarity" has been given numerical meaning. "Identical" observations are 100% similar while "totally dissimilar" observations are 0% similar or have zero similarity. Of course, there is a continuous range between these two extremes.

Geometrically each observation (sample) can be considered as a point in a multidimensional space. Each dimension represents a variable (element). In this multidimensional space, samples which have similar overall compositions will form a cluster of points. Therefore, groups may be formed by calculating all of the possible distances between pairs of points. Then, based on these distances, a cluster that happens to have short inter-point distances is considered a group. The distance between two samples can be calculated by various ways [8], the Euclidean distance, will be used in this analysis.

The Euclidean distance is the square root of the sum of the squares of the differences in the concentration, of each element in two samples. It is stated mathematically by:

$$D_{x,y} = \sqrt{\sum_{i=1}^M (x_i - y_i)^2}$$

where

$D_{x,y}$ = Euclidean distance between the two samples x and y .

M = number of elements determined.

x_i = concentration of the i^{th} element in the sample x

y_i = concentration of the i^{th} element in the sample y

Standardization of the data (concentration of the elements) has an important role in clustering especially when the clustering technique uses the Euclidean distance [18]. Therefore, the data were standardized to zero mean and unit variance before actual manipulation started by means of a method known as the CLUSTER PROCEDURE.

The first step in the clustering analysis is the formation of the distance matrix, the elements of which are the distances between every pair of samples as calculated by using the Euclidean distance equation. The clustering procedure then fuses samples or groups of samples which are close (or most similar) [19], i.e., which have low inter-point distances. The clustering procedures used in this study are of an agglomerative hierarchical type. Each observation (sample) begins in a cluster by itself. Then the two closest clusters (single point or samples in this case) are merged into one cluster replacing the two original ones. Next, two clusters, selected because the distance between them is small, are joined. It is to be noted that these two clusters may be single point clusters (samples) or the first joined cluster and a third single point. This merging is repeated until only one large cluster is left [18,19,23].

The grouping procedures used in this study are the 1982 revised

version of the package called "CLUSTER PROCEDURES" available from SAS Institute Inc., Cary, North Carolina [37]. This code uses three standard agglomerative hierarchical clustering algorithms (Centroid Method, Ward's Method, and Average Linkage Method). The difference between the three algorithms resides in the way the distance between two clusters is computed.

i) The centroid method - In this case the distance between the two clusters is simply defined by the Euclidean distance between their centroid or means. This method does not perform as well as the other two methods, however, it is more responsive to distant points than are other hierarchical methods [37].

ii) The average linkage method, in which the distance between the two clusters is defined to be the average distance (Euclidean) between pairs of samples (one from each cluster). Mathematically, the cluster distance is

$$D_{w(xy)} = [\sum_i \sum_k D_{ik}] / N_{(xy)} N_w$$

where:

D_{ik} = Euclidean distance between sample i in the cluster xy and sample k in the cluster w .

$N_{(xy)}$ = number of samples in cluster xy

$N_{(w)}$ = number of samples in cluster w [23]

The average linkage method tends to combine clusters with small variances and is biased towards producing clusters with approximately the same variances [37].

iii) The Ward's method - In this case, the distance between two clusters is simply the sum of squares between the two clusters added up over all variables. In each generation, or iteration, the "within - cluster" sum of squares is minimized over all partitions which are obtained by joining two clusters from the previous generation. Although Ward's method is biased toward producing cluster with approximately the same number of samples, it tends to combine clusters having small numbers of samples [37].

Even though hierarchical clustering does not have any provision for a relocation of samples that may have been wrongly grouped at an early stage, the use of different clustering methods can uncover a natural grouping if the outcomes from these methods are roughly consistent [18,23].

The most convenient way of presenting the results of a clustering procedure is a clustering tree, or dendogram. In Figure 5, the ends of the branches at the right represent the individual samples. As one moves to the left, these branches join to form clusters. At the far left all clusters are joined to form the final single cluster. Therefore, from inspection of the dendogram one observes the existing groups at a given vertical level and the associated dissimilarity on the horizontal axes. The later ranges from zero (totally similar) to unity (completely dissimilar). Separate clusters at different dissimilarity levels (or values) can be obtained by slicing the dendogram with a vertical line at that particular value.

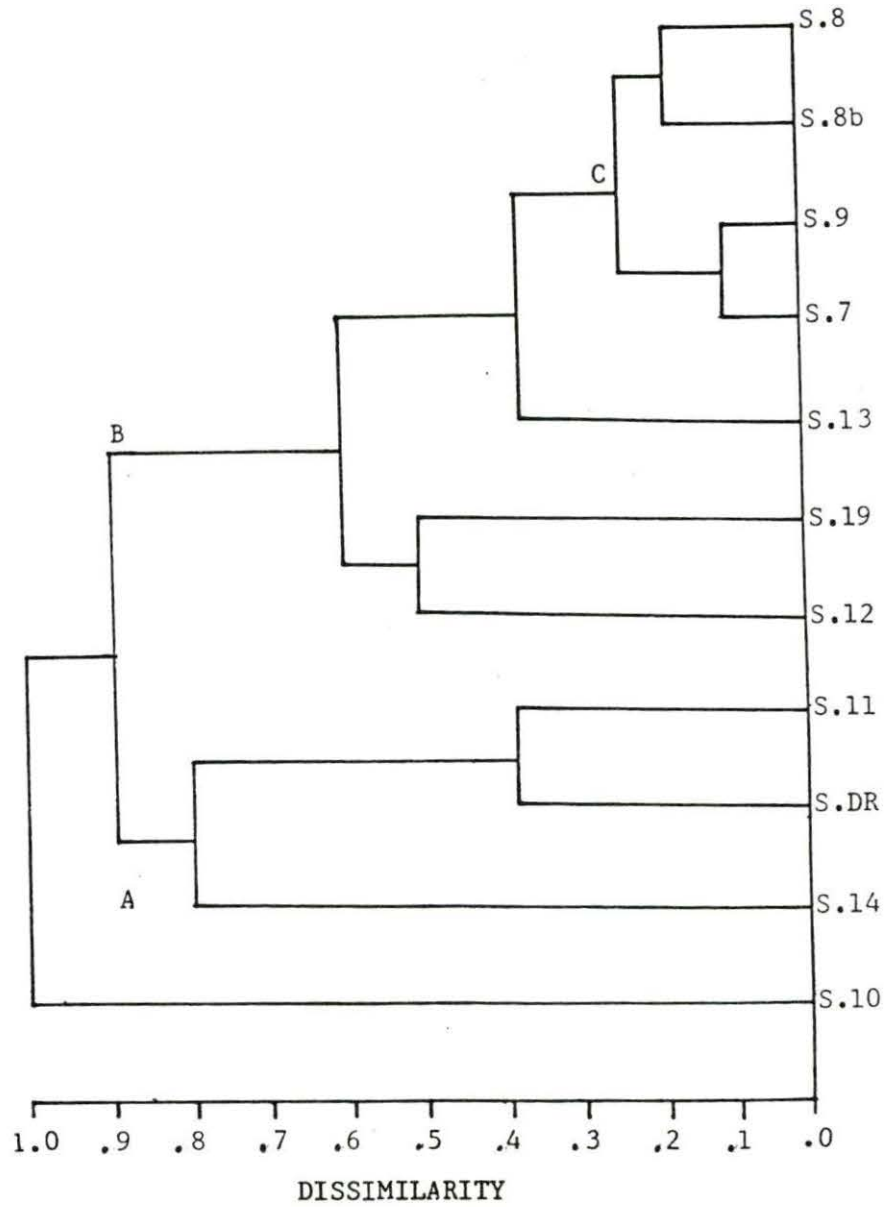


Figure 5. Dendrogram resulting from centroid method

3.1.2. Group Refinement

In Bieber's study [8], the refinement of the groups was achieved by using the MAHALANOBIS distance technique. Unfortunately, this distance cannot be calculated when the number of group members is less than the number of elements used. This inconvenience limits the use of this technique to the following cases:

- Large groups with every element determined, or
- Small groups with the exclusion of several elements from the analysis.

Since the available data cannot be altered, the above technique was discarded. The alternative was to visually inspect the concentration curves for the different samples, and compare them to each other.

In carrying out the visual inspection, the first step was to normalize the concentration of each element in the sample by the corresponding concentration of the same element in sample #11. In the second step the concentration curves for each element were plotted on a "transparency" to facilitate the comparison. As one can see in Figure 8, the abscissa of the plots represents the element identification number (see Table 5), whereas, the ordinate shows the relative concentration. Furthermore, for purposes of simplicity, each concentration curve was plotted as a continuous curve, so that various patterns associated with different groups can be identified at a glance. It will be observed that not all of the of normalized standard deviations are shown in the curves. This is due to the fact that this quantity (normalized standard deviation) was found to be very small, except for Sm-153, Yb-175, Rb-86, Sr-85, Nd-147, and Sb-122. Therefore, not all of the normalized

deviations were shown on the curves. Third, superimposing these curves over a light source allows further discrimination of the clustering results.

3.2. Formation of Groups

The variables used in the Clustering technique consist of all the twenty-five elements shown in Table 2 and which are to be found in all the samples.

a) The dendogram resulting from the Centroid Cluster Technique (Figure 5) shows three main groups, two multisamples and one unisample.

The unisample group is totally dissimilar to the other two groups which are 10% similar. Those two are groups A and B. Group A consists of sample 14 and a cluster (DR and 11). Group B is composed of two subgroups b_1 and b_2 . The b_1 subgroup includes samples 12 and 19 while b_2 consists of sample 7, 9, 8, 8b, and 13. From the dendogram, one observes that group A is loose, i.e. it is formed at a high level of dissimilarity whereas the B group is tight.

b) Clustering by the Average Linkage Method under the same conditions produced three main clusters as in the centroid cluster technique (Figure 6). One unisample (sample 10) and two multisamples (Group A and B).

In spite of the similarity of the two dendograms, the looseness and tightness of the groups are slightly changed. This is due to the differences between the two techniques.

c) The Ward's Clustering Method dendogram (see Figure 7) shows what may seem, at first, to be a different result. Only two main groups are

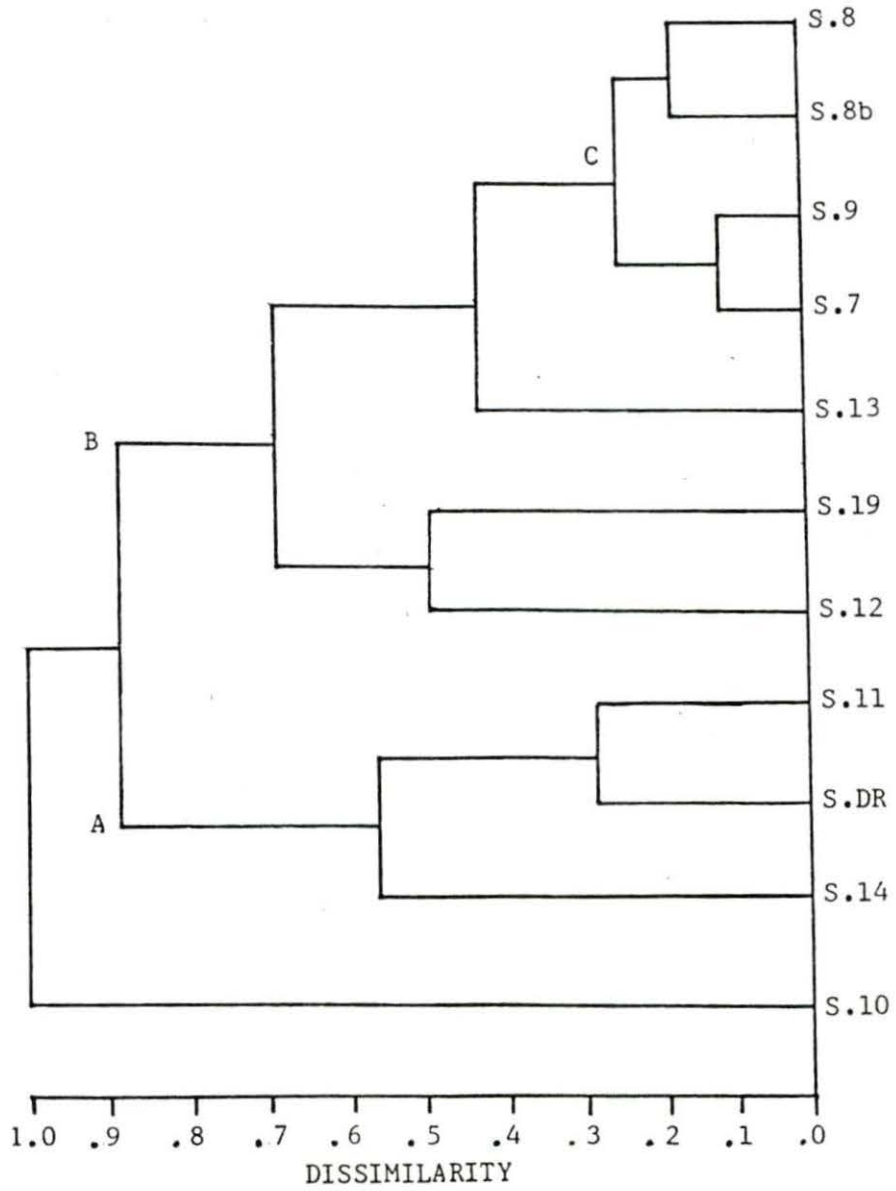


Figure 6. Dendrogram resulting from average linkage method

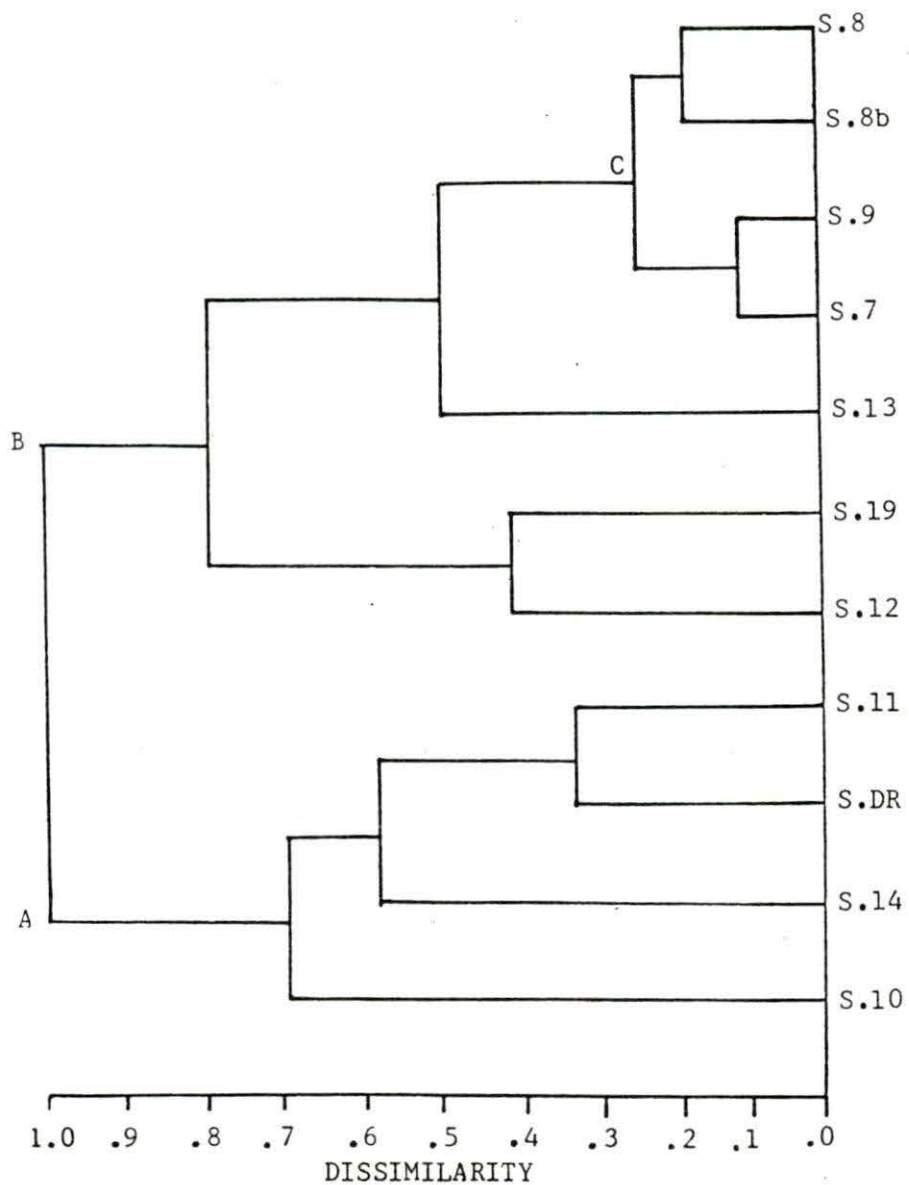
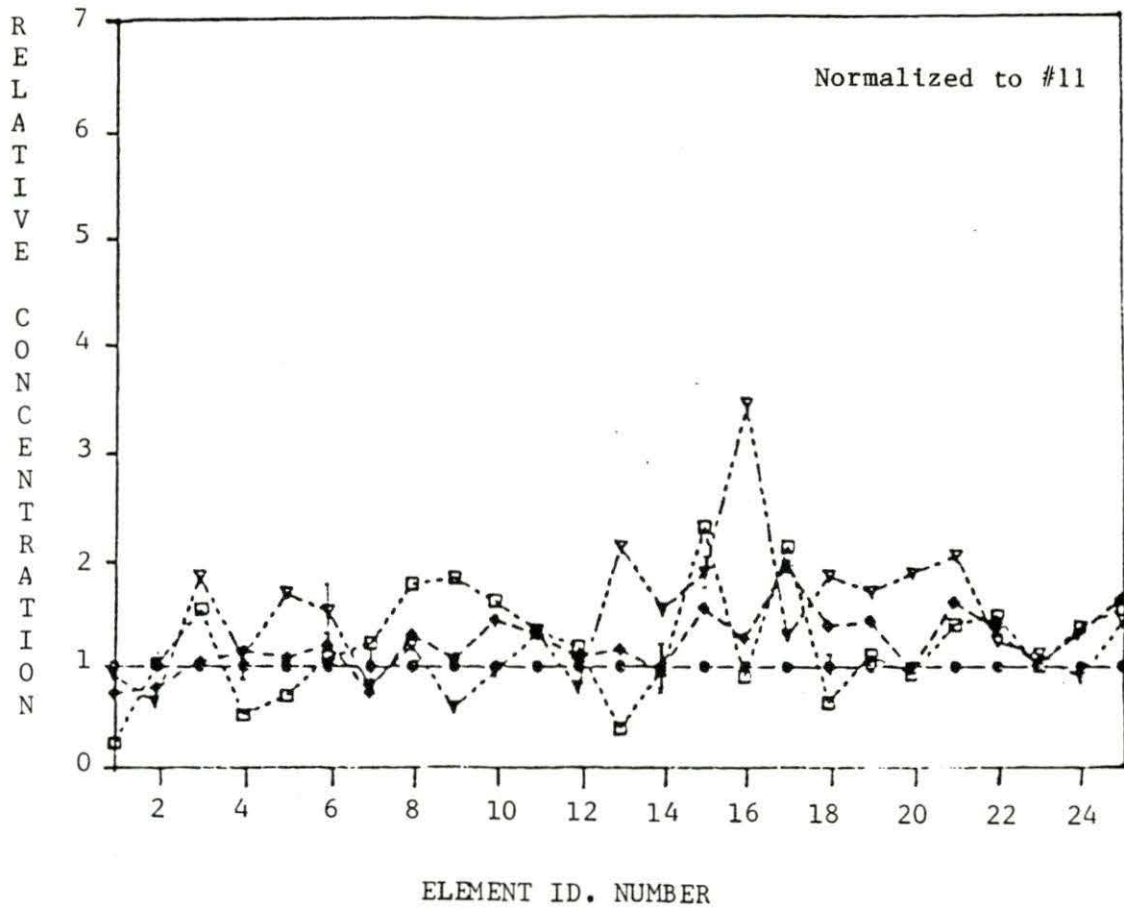


Figure 7. Dendrogram resulting from Ward's Method



Key: Sample # 10 ▽-▽
 Sample # 11 ○-○
 Sample # 14 □-□
 Sample # DR ◇-◇

Figure 8. Relative concentration curves for samples 10, 11, 14, and DR

identified. Actually this result is the same as for the three groups found before. Here, group A consists of sample 10 merged with the cluster (DR, 11 and 14) which is equivalent to group A in the other dendograms (Figures 5 and 6). Group B includes samples 7, 9, 8, 8b, 13, 12, and 19. Moreover, the tightness/looseness of the Ward's dendogram characterizes this method. Although different levels of dissimilarity show different number of groups in the three dendograms, there is a consistency in the net result. This supports the validity of the classification.

The dissimilarity level used to separate groups or samples with experimentally determined resemblances as being similar or dissimilar is found by comparing the information found in the concentration curves. Starting with samples 10, 14, DR, and 11 (Figure 8) we can notice that there is no apparent compositional patterns that would indicate any kind of similarity between the samples. This confirms the tentative conclusion reached using the grouping method. Therefore these samples have different origins.

The comparison of samples 7, 9, 8, 8b, 13, 12, and 19 (the second major group, B) reveals a general similarity in the concentration patterns with some variations (see Figure 9). In the cases of samples 8 and 8b (Figure 10), the concentration levels of twelve elements agreed within one standard deviation, while six others (three and three) agree within two and three standard deviations, respectively, (Table 4). In the case of samples 7 and 9 (Figure 11), nine elements have the same concentration within one standard deviation. Five more elements agree within two standard deviations and three others within three standard

deviations. These elements are listed in Table 4. Consequently, from the results found in three dendograms and from the concentration arguments presented above, one can support the opinion that samples 7, 8, 8b, and 9 have the same origin as summarized in the following points:

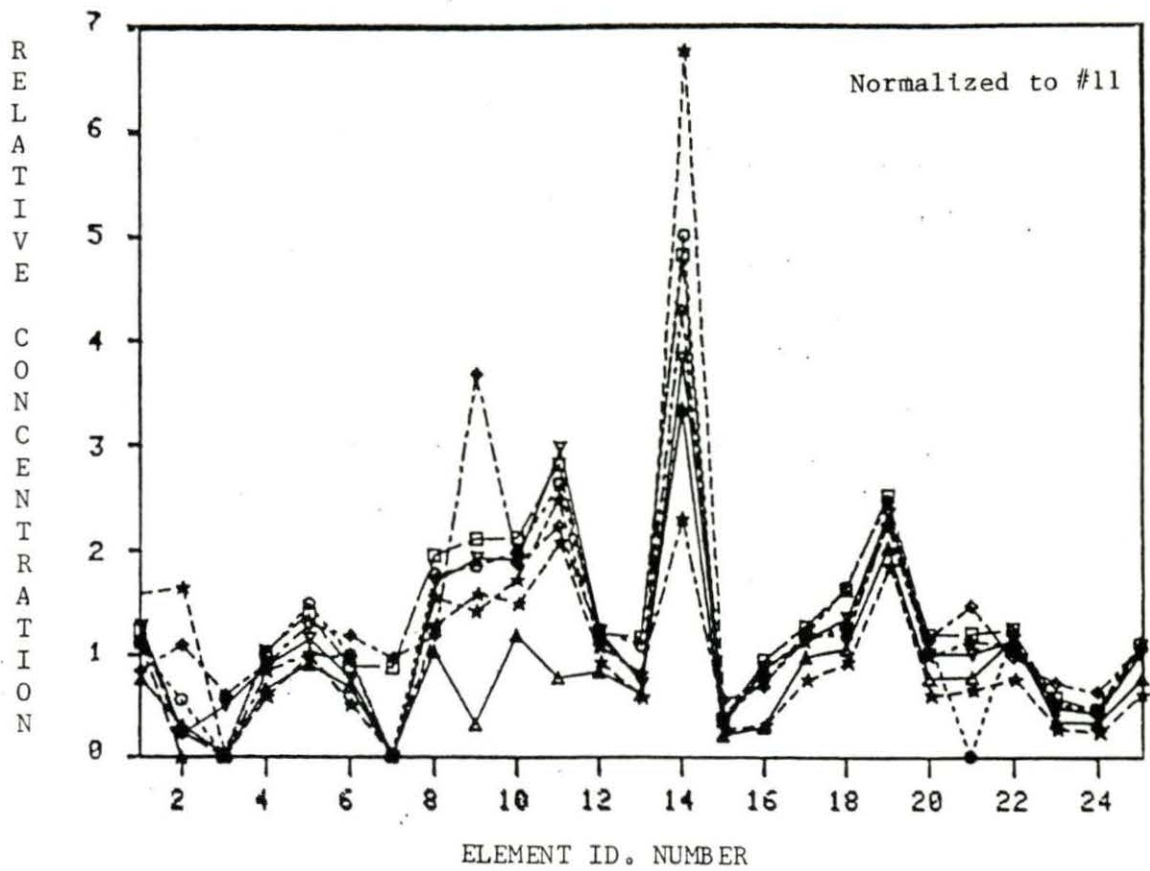
- the clustering results show a 76% similarity between the samples,
- The uniformity of their concentration curve patterns which is disturbed only by the contributions from four elements (see Figure 12). These are elements no. 5, 9, 13, and 14 (Sm-153, Cr-51, Rb-86, and Sr-85), and were selected because their percentage standard deviation exceeded 15.5% see (Table 5).

The comparison of sample 13 with the cluster C (Figures 13a and 13b) show:

- the concentrations of elements 2, 9, and 21 (As-76, Cr-51, and Yb-169) in this sample are greater than the range of concentrations for the corresponding elements in group C, while

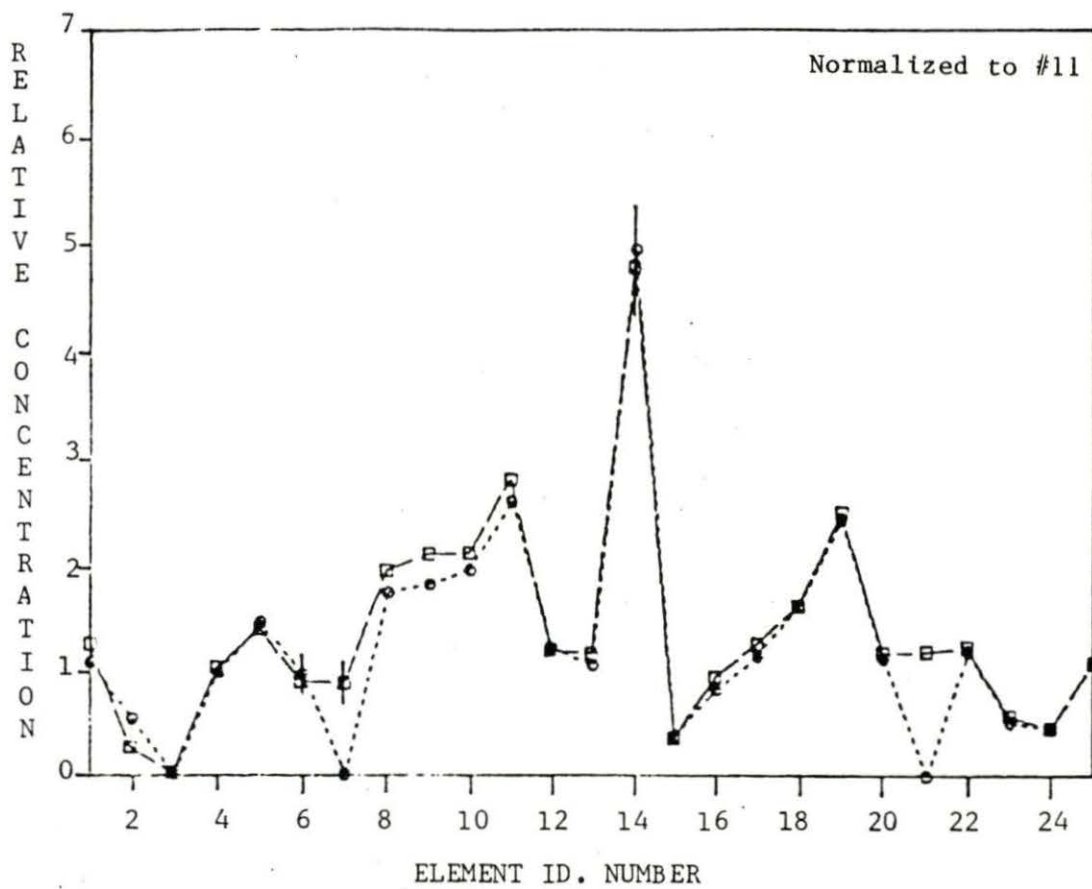
- the concentration of elements 1, 8, 11, and 18 (Na-24, Sc-48, Co-60, and Nd-147) are less.

A different kind of variation in the curves can be recognized in the case of samples 12 and 19. The concentrations of most of the elements present in sample 12 is below the range (group C) by a factor ranging from .6 to .5 Figure 14a and 14b. However, the concentrations of elements 1, 2, and 14 are above the range by the reciprocal of .5 and .6 (1.5 and 2). This shift could be produced by the introduction of a certain amount of impurities into the averaged composition of the samples which comprise C cluster. Actually this could be achieved by the deliberate addition of a fixed amount of "temper" (Material added by the



Key: Sample # 7 ▽-▽
 Sample # 8 □-□
 Sample # 8b ○-○
 Sample # 9 ★-★
 Sample # 12 ★-★
 Sample # 13 ◇-◇
 Sample # 19 △-△

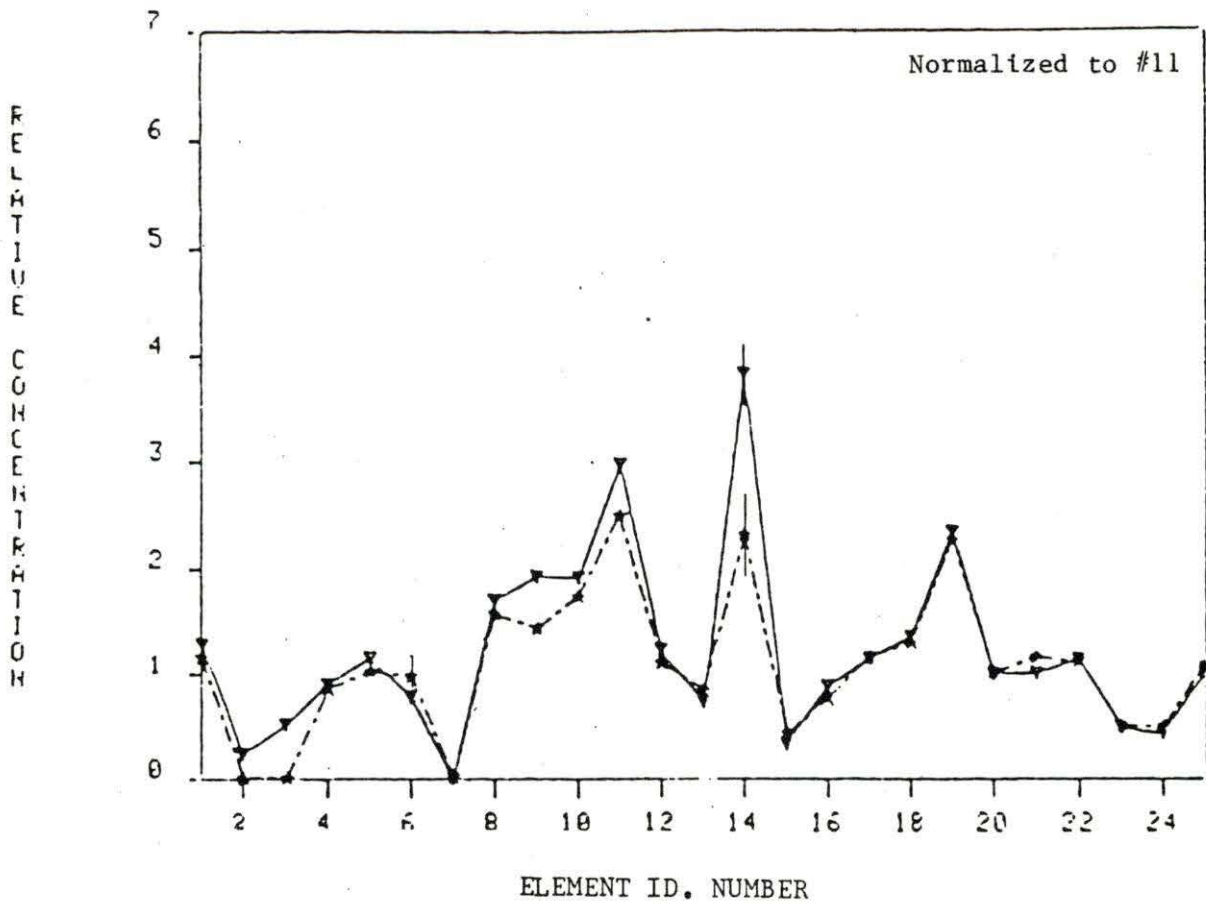
Figure 9. Relative concentration curves for sample 7, 8, 8b, 9, 12, 13, and 14



Key

Sample # 8b ○---○
 Sample # 8 □---□

Figure 10. Relative concentration curves for samples 8 and 8b



Key

Sample # 7 ▽—▽
Sample # 9 ★—★

Figure 11. Relative concentration curves for samples 7 and 9

Table 4. The common elements between samples 8 and 8b and samples 7 and 9, respectively

Samples	1	2	3
8 & 8b	Lu-177 Th(Pa-233) Hf-181 Tb-160 Eu-152 Nd-147 Sb-124 Sr-85 Rb-86 Zn-65 Yb-175 Sm-153	Ta-182 Co-60 La-140	Cs-134 Sc-46 Na-24
7 & 9	Ln-177 Ta-182 Hf-181 Tb-160 Eu-152 Nd-147 Sb-124 Yb-175 Sm-155	Yb-169 Ce-141 Rb-86 Zn-65 La-140	Cs-134 Sr-85 Na-24

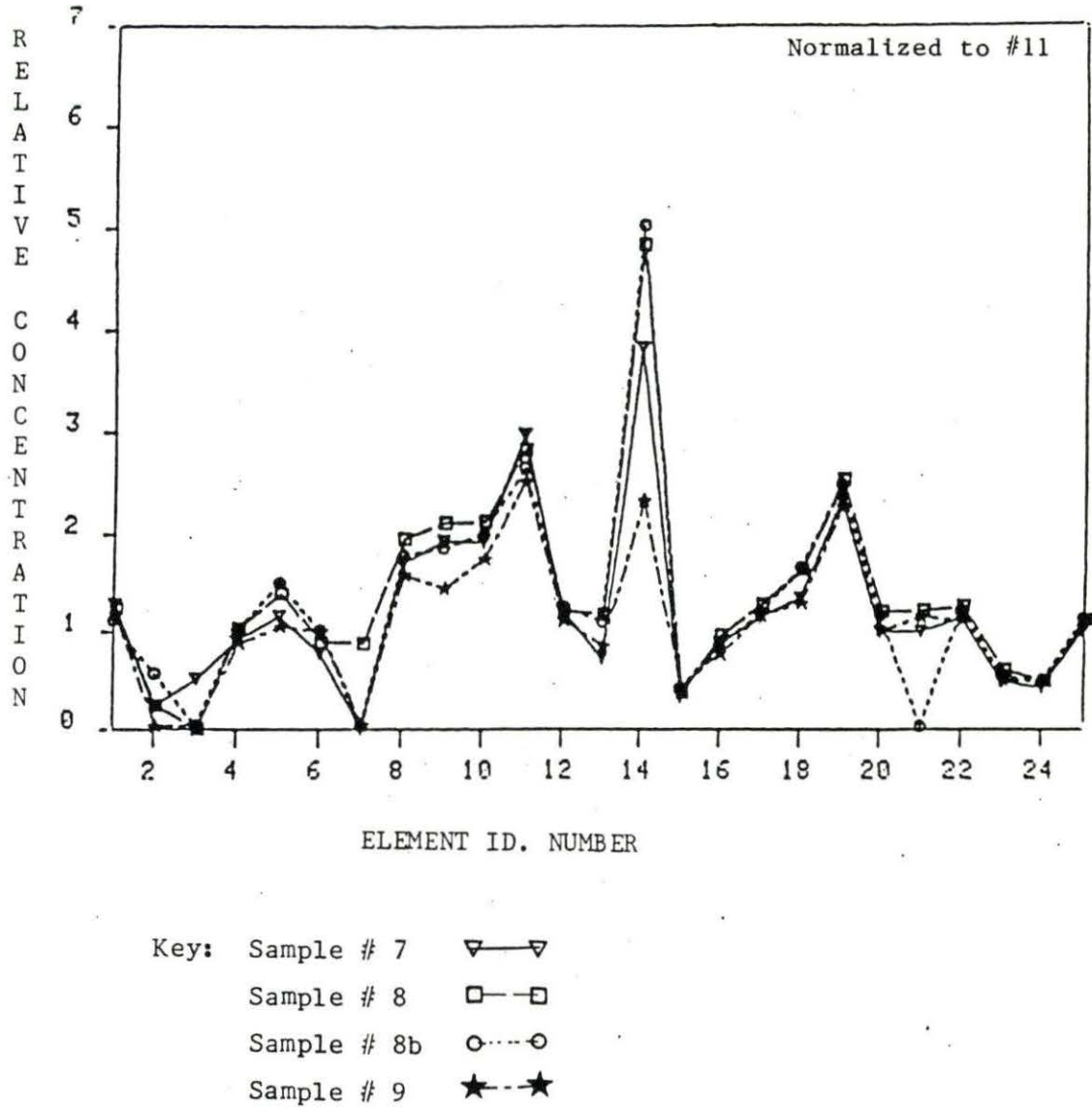


Figure 12. Relative concentration curves for samples 7, 8, 8b, and 9

Table 5. Mean concentration of 7, 8, 8b, and 9--Xachimilco collection (concentration in ppm except for Na and Fe in % x 10⁴)

I.D.N	Elements	Mean	σ	%
1	Na-24	10306.875	803.8	7.8
2	As-76	-*	-*	-*
3	Sb-122	-*	-*	-*
4	La-140	26.019	2.5	9.4
5	Sm-153	6.003	.99	16
6	Yb-175	2.74	.28	10.2
7	U(Np-239)	-*	-*	-*
8	Sc-48	14.66	1.4	9.4
9	Cr-51	99.56	16.0	16.1
10	Fe-59	41554.67	3123.5	7.5
11	Co-60	16.97	1.4	8.1
12	Zn-65	84.13	4.9	5.8
13	Rb-86	69.58	15.6	22.3
14	Sr-85	431.43	135.2	31.3
15	Sb-124	.4758	.039	9.0
16	Cs-134	3.73	.39	09.4
17	Ce-141	52.74	.397	1.5
18	Nd-147	30.64	4.01	13.09
19	Eu-152	1.585	.081	5.11
20	Tb-160	.891	.084	9.43
21	Yb-169	-*	-*	-*
22	Hf-181	5.924	.37	6.21
23	Ta-182	.673	.0688	10.23
24	Th(Pa-233)	5.91	.3	5.08
25	Lu-177	.339	.014	4.19

* at least one of the four samples yielded a concentration = 0

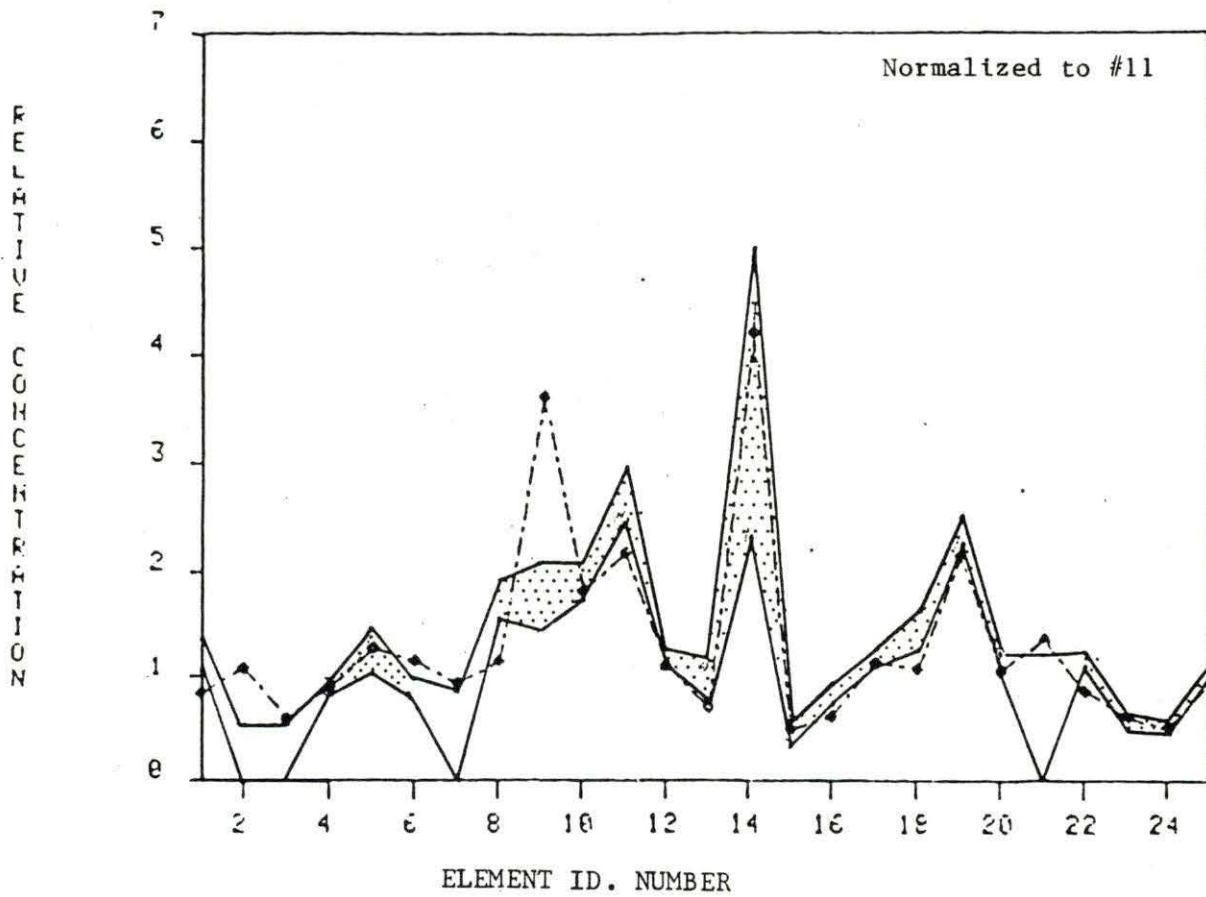


Figure 13a. Relative concentration curves for sample 13 compared to the concentration range of the group C

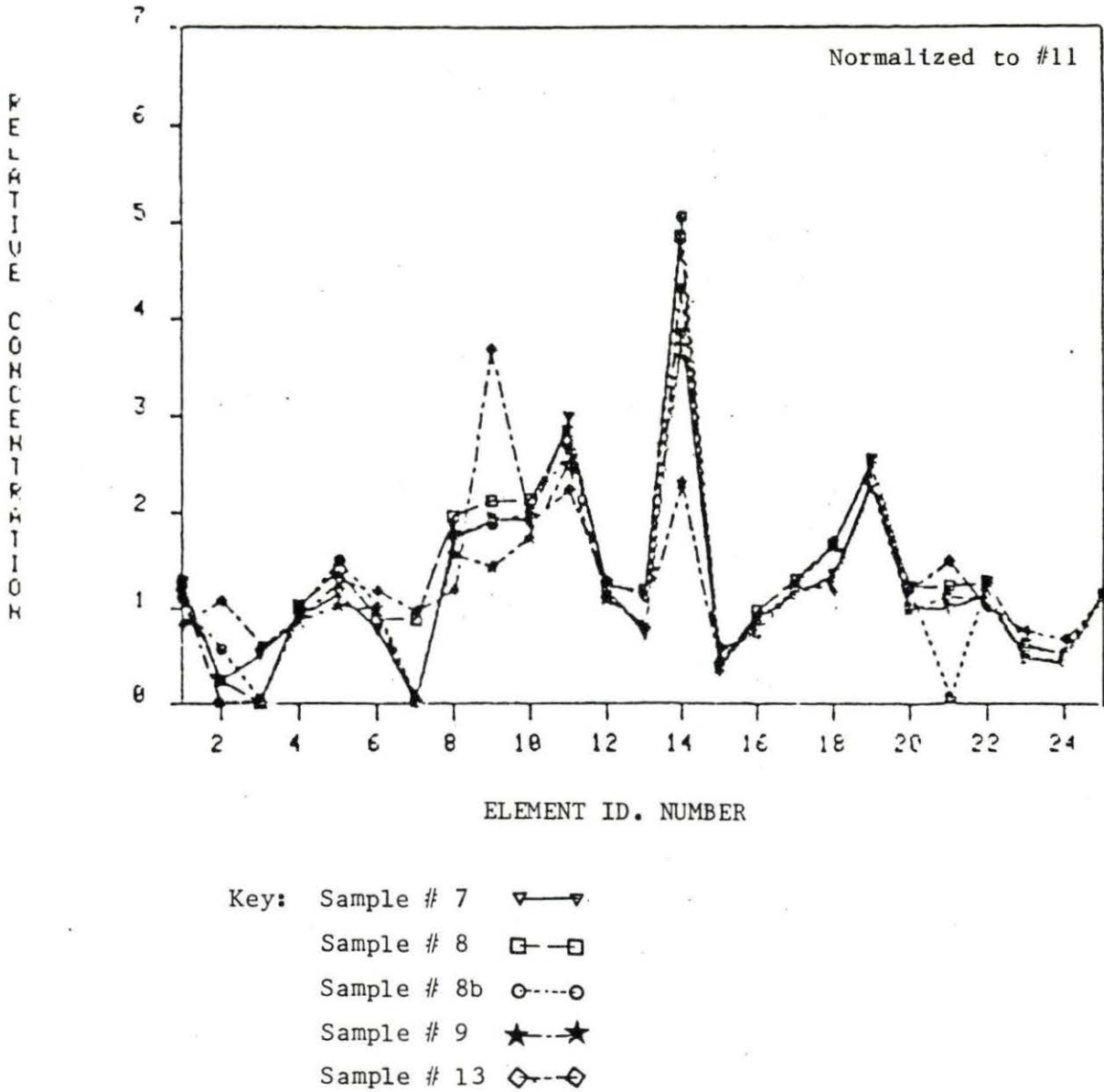


Figure 13b. Relative concentration curves for sample 13 compared to samples 7, 8, 8b, and 9 (group C)

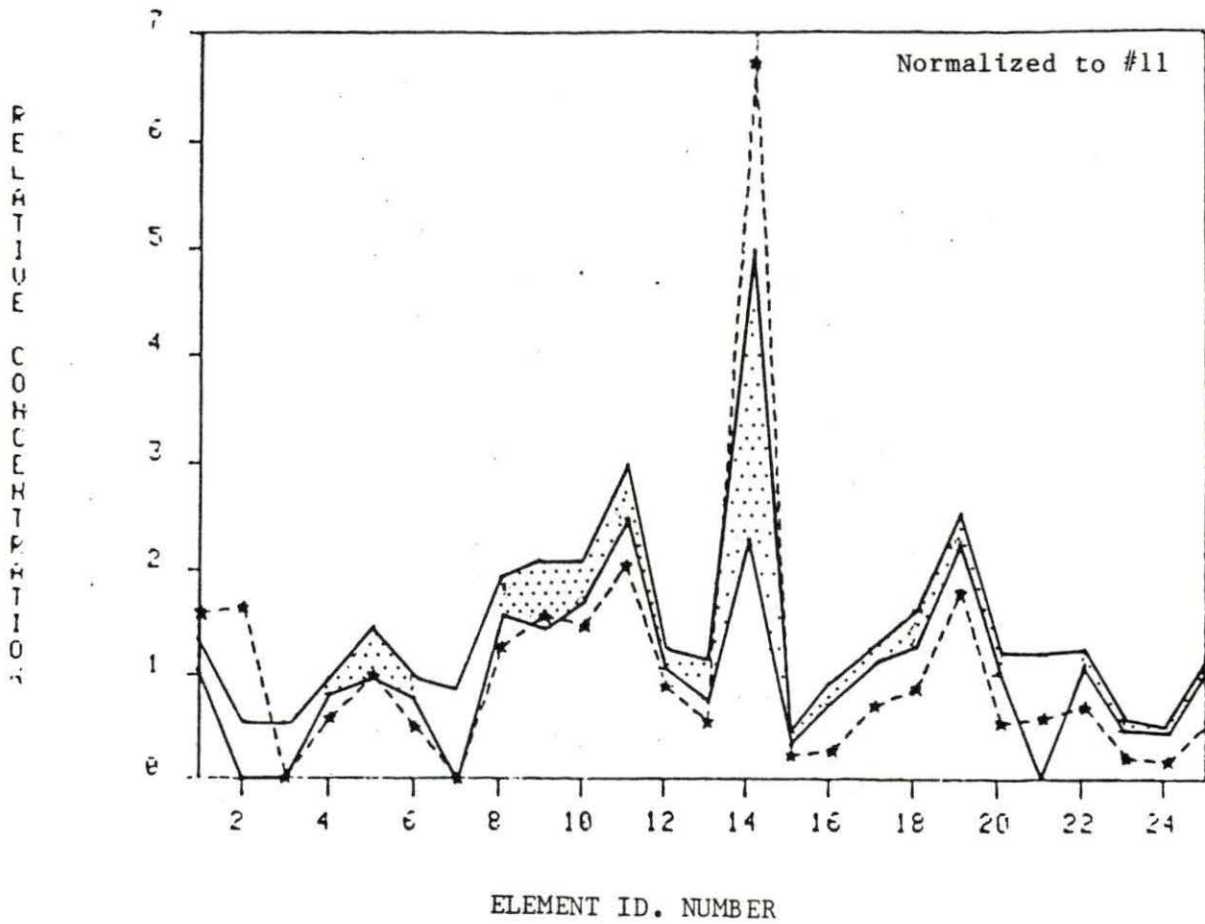
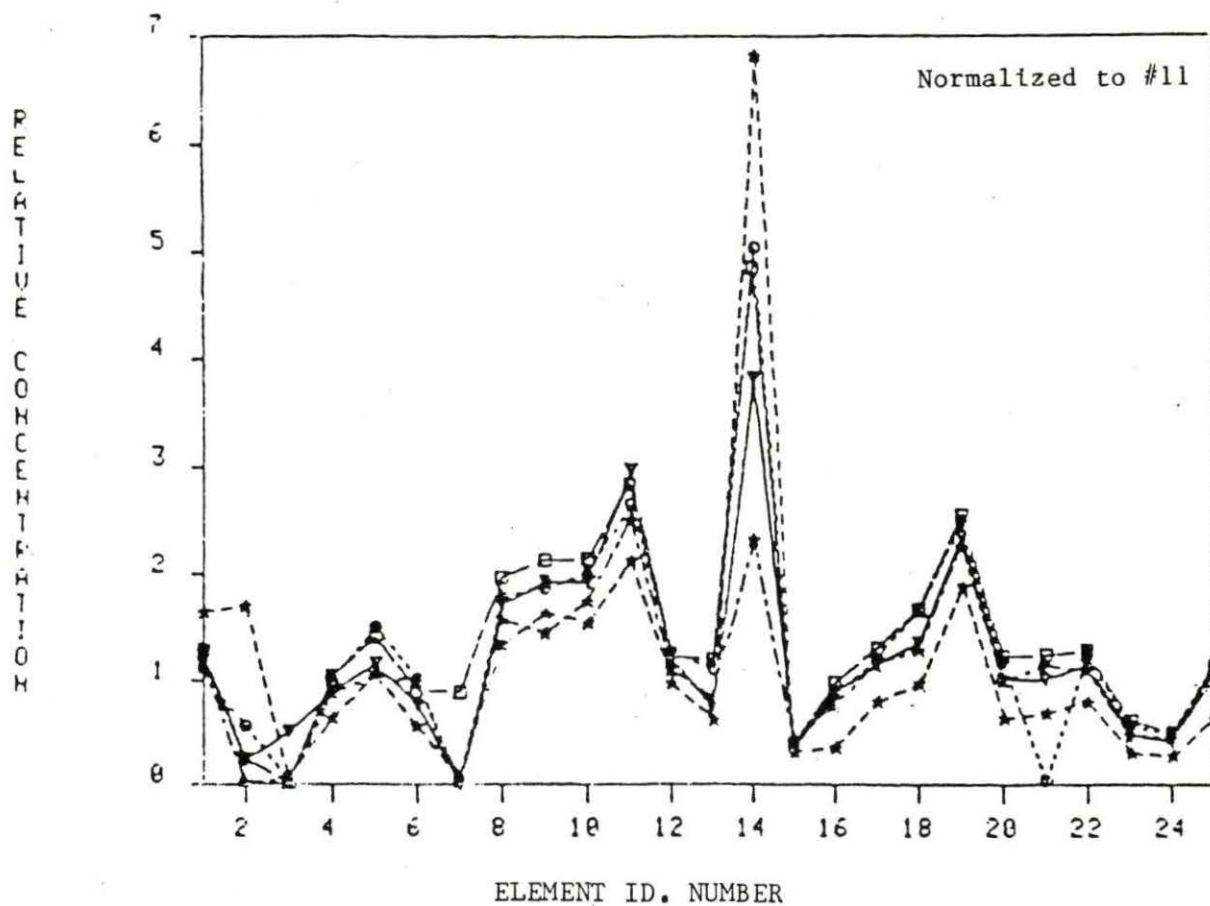


Figure 14a. Relative concentration curves for sample 12 compared to concentration average of the group C



Key:

- Sample # 7 ▽—▽
- Sample # 8 □—□
- Sample # 8b ○—○
- Sample # 9 ★—★
- Sample # 12 ★—★

Figure 14b. Relative concentration curves for sample 12 compared to samples 7, 8, 8b, and 9 (group C)

potter to achieve certain desired effects) into the clay paste. Furthermore, in the case of sample 19, all the concentrations are less than the range by a factor ranging from .5 to .8, except for elements (9, 8, and 11) which distinguish the sample 19 pattern from the average one (see Figures 15a and 15b). Since the absence of these elements cannot be explained by the addition of temper, it is speculated that this sample represents a unique clay bed.

Finally, although the cluster B consists of samples with similar concentration patterns, it is hard to define more than one multisample group (group C) or to join to it any other sample. Nevertheless, sample 12 can be added to the group with the precaution that it could be of different origin. Thus more information about the different clay beds are needed to settle such problems.

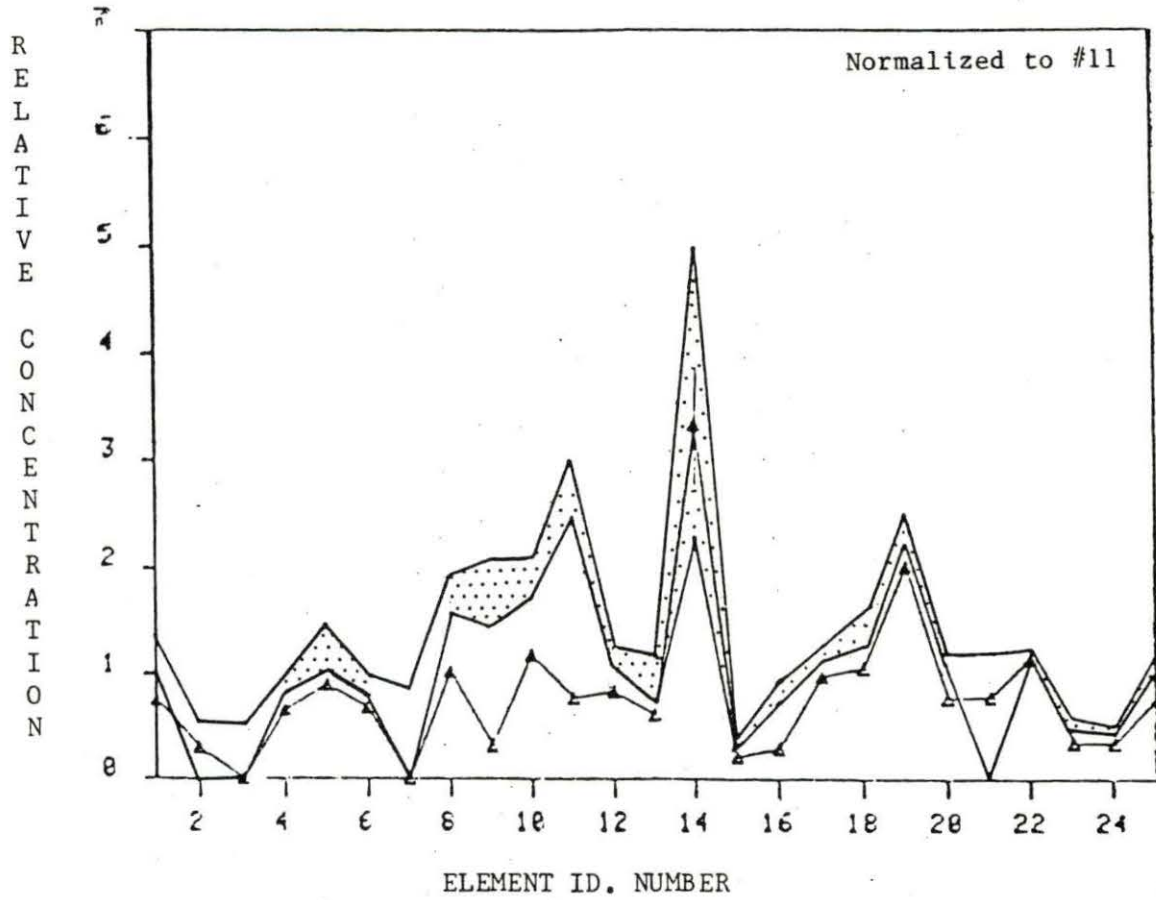
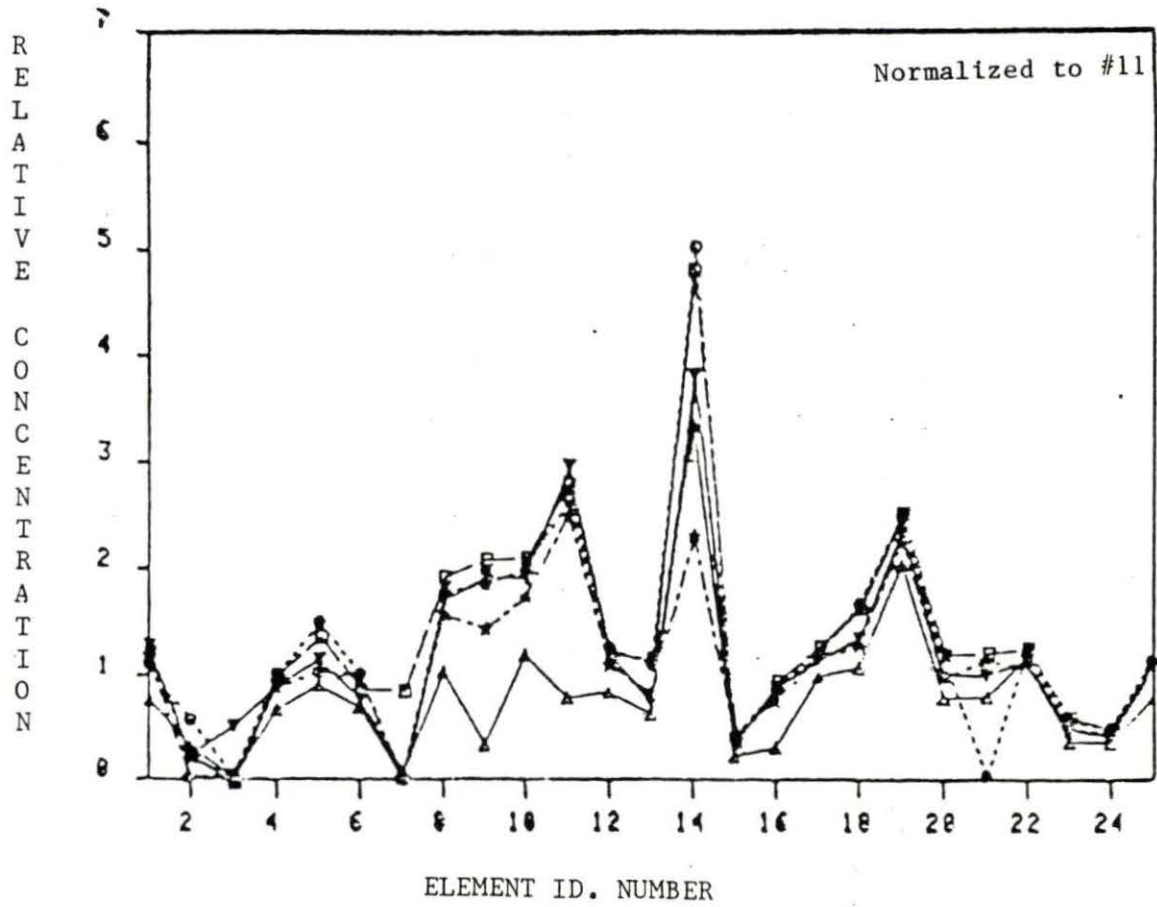


Figure 15a. Relative concentration curves for sample 19 compared to the concentration range of the group C



Key:

Sample # 7	▼—▼
Sample # 8	■—■
Sample # 8b	○-○
Sample # 9	★-★
Sample # 19	▲—▲

Figure 15b. Relative concentration curves for sample 19 compared to samples 7, 8, 8b, and 9 (group C)

4. CONCLUSIONS

4.1. Archaeological Implications

This investigation was devoted to studying similarities between the Mexican pottery (samples). The results revealed the following:

- the collection (samples 7, 8, 8b, 9) from Santa Cruz Acalpixa, Xachimilco appeared to have the same origin, the same clay bed.
- the Edzna, Campeche collection (samples 10, 11, and 12) showed a total contrast between its samples.
- the Chiapa de Corzo, Chiapas collection (samples 13 and 19) looked different. However,
- sample 12 (from Edzna, Campeche) was found to match the Xachimilco collection.

The above observations indicate that every sample from Campeche and from Chiapas represent different clay beds. This implies either or both of the following:

- within each center, or location, there is a number of different clay beds used for manufacturing the potshards examined. Or
- not all of potshards within the collection are locally made; this would indicate the existence of trade patterns.

Moreover, the observations showed that sample 12, from the Campeche collections, matches the Xachimilco collection. Thus, one can conclude that

- the Xachimilco collection and sample 12 of Campeche could be produced in either center and then transported to the other. Or
- the collection and the sample were made at a third place (center) and then moved to where it was found.

4.2. Direction for Future Work

In order to clarify the nature of each center and its relationship to the others, samples from the local clay beds within each center should be analyzed and compared. Also, more potshards samples from the different centers should be investigated. Thereafter, definite archaeological statements can be given.

Mineralogical examination (X-ray diffraction) of inclusions in the ceramic and clay beds fabric [30] could, when combined with neutron activation analysis, clarify the relationship between tempered and untempered pottery made from the same clay. Such a study might define the relationship between sample 12 and the Xachimilco collection.

Compared to the understanding which exists about Mediterranean and Meso-American pottery, the study of Mexican pottery is in an early stage. The present work is a contribution. Obviously, much more work needs to be done before significant results become evident. However, the work at hand sheds some light on the probable relationship between two centers. This emphasizes once again the great promise that application of physical science to archaeology holds.

REFERENCES

1. Abascal, R. M., G. Harbottle, and E. V. Sayre. 1974. Correlation between Terra Colta Figurines and Pottery from the Valley of Mexico and Source Clays by Activation Analysis. *Adv. in Chem.* 138:81-99.
2. Al-Ketal, R. A., L. H. Chan, and E. V. Sayre. 1969. Neutron Activation Analysis of Pottery from Hajar Bin Humeid and Related Areas. Appendix II in G. W. Van Beek. *Hajar Bin Humeid: Investigations of a Pre Islamic Site in South Arabia.* Johns Hopkins Press, Baltimore, Md. 387 pp.
3. Amiel, S. 1981. *Nondestructive Activation Analysis.* Elsevier Scientific Publishing Company, Amsterdam.
4. Artzy, M., F. Asaro, and I. Perlman. 1973. The Origin of the "Palestinian" Bichrome Ware. *J. Am. Oriental Society* 446-461.
5. Attas, M., L. Yaffe, and T. M. Fossey. 1977. Neutron Activation Analysis of Early Bronze Age Pottery from Lake Vouliagmeni. Perakhora, Central Greece. *Archaeometry* 19, 1:33-43.
6. Beek, J. O., J. Putman, R. Gijbels, J. DeDandey, and J. Hoste. 1976. Similarity Analysis of Pottery Based on Neutron Activation Analysis Data. *Proc. of Intern. Conf. on Application of Nuclear Methods in the Field Works of Arts.* Academia Nazionale Dei Lincei, Rome. 47 pp.
7. Bennyhoff, J. A., and A. F. Heizer. 1965. Neutron Activation Analysis of some Cuicuilco and Teotihuacan Pottery, Archaeological Interpretation of Results. *Am. Antiq.* 30:348-349.
8. Bieber, A. M., D. W. Brooks, G. Harbottle, and E. V. Sayre. 1975. Compositional Grouping of Some Ancient Aegean and Eastern Mediterranean Pottery. *Proc. of Intern. Conf. on Applications of Nuclear Methods in the Field Work of Arts.* Academia Nazionale Dei Lincei, Rome. 113 pp.
9. Birgul, D., M. Diksic, and L. Yaffe. 1977. Activation Analysis of Turkish and Canadian Clays and Turkish Pottery. *J. Radioanal. Chem.* 39:45-62.
10. Boule, G. J., and M. Persach. 1977. Characterization of South West African Potsherds by Neutron Activation Analysis of Trace Elements. *J. Radioanal. Chem.* 39:33-44.
11. Brooks, D., A. M. Bieber, G. Harbottle, and E. V. Sayre. 1974. Biblical Studies Through Activation Analysis of Ancient Pottery. *Adv. in Chem.* 138:48-80.

12. Bureau of Radiological Health. 1970. Radiological Health Handbook. Bureau of Radiological Health, Rockville, Maryland. 217 pp.
13. Cooper, R. D., and G. L. Brownell. 1967. Neutron and Bremsstrahlung Activation Analysis. MIT Dept. of Nuclear Eng. Report MITNE 82:80-92.
14. CRC Handbook of Tables for Applied Engineering Science. 1970-1973. 2nd ed. CRC Press Cleveland, Ohio.
15. CRC Handbook of Chemistry and Physics. 1983-1984. 64th ed. CRC Press Cleveland, Ohio.
16. Czerng, W., and G. Winkler. 1977. Nondestructive Activation Analysis of Ancient Pottery by 14 MeV Neutrons. J. Radioanal. Chem. 40:165-173.
17. Diebolt, J., and J. C. Rica. 1977. An Attempt to Select Suitable Elements to Characterize An Ancient Ceramic by Neutron Activation Analysis. J. Radioanal. Chem. 19:9-20.
18. Everilt, B. S. 1977. Cluster Analysis. Heinemann Educational Books Ltd, London.
19. Everilt, B. S. 1978. Graphical Techniques for Multivariate Data. Heinemann Educational Books Ltd., London.
20. Glascock, M. D. 1983. Neutron Activation Analysis Tables. Unpublished. Univ. of Missouri, Columbia, Mo.
21. Grimanis, A. P., M. V. Crimani, and M. I. Kovayannis. 1977. Instrumental Neutron Activation Analysis of Melian Potsherds. J. Radioanal. Chem. 39:21-31.
22. Johanson, R. A., and F. H. Stross. 1965. Laboratory Scale Instrumental Neutron Activation for Archaeological Analysis. Am. Antiq. 30:345-347.
23. Johnson, R. A., and D. W. Wichern. 1982. Applied Multivariate Statistical Analysis. Prentice-Hall, Englewood Cliffs, New Jersey. 533 pp.
24. Joron, J. L., M. Treuil, and H. Jaffrezic. 1977. Trace Element Archaeochemistry in Different Sigillared Potteries, Using Neutron Activation Analysis. J. Radioanal. Chem. 39:63-67.
25. Knoll, G. F. 1979. Radiation Detection and Measurement. J. Wiley and Sons Press, New York. 423 pp.
26. Lyon, W. W. 1982. Practical Application of Activation Analysis and other Nuclear Techniques. Department of Energy Report DE82 009479.

27. Maddin, R. and J. D. Muhly. May 1974. Some Notes on the Copper trade in the Ancient Mid-East. *J. Metales* :24-30.
28. National Geographic Society. 1981. *Atlas of the World*. Washington D.C. 114 pp.
29. Olin, J. S. and E. V. Sayre. 1971. Compositional Categories of English and American Pottery of the American Colonial Period. Chapter 14 in R. H. Brill, ed. *Science and Archaeology*. MIT Press, Cambridge, Mass.
30. Peacock, D. P. S. 1970. The Scientific Analysis of Ancient Ceramic: A Review. *World Archaeology* 1:375-388.
31. Perlman, I. 1981. Application to Archaeology. Pages 259-279 in S. Amiel, ed. *Nondestructive Activation Analysis*. Elsevier Scientific Publishing Co., Amsterdam.
32. Perlman, I, and F. Asaro. 1967. Deduction of Provenience of Pottery from Trace Element Analysis. Report UCRL-17937. Lawrence Radiation Laboratory, Berkeley, CA.
33. Perlman, I. and R. Asaro. 1969. Pottery Analysis by Neutron Activation. *Archaeometry* 11:21-52.
34. Price, W. J. 1964. The Geige-Muller Counter. Chapter 5 in W. S. Price, ed. *Nuclear Radiation Detection*. McGraw-Hill Book Co., New York.
35. Rakovic, M. 1970. *Activation Analysis*. Translated by D. Cohen. Iliffe Books LTD, London.
36. Romberg, W. D. 1969. Impurities in MGC by Instrumental Neutron Activation Analysis. Thesis. ISU, Ames, Iowa.
37. SAS Institute. 1982. *SAS User's Guide for Statistics*. SAS, Cory, North Carolina. 423 pp.
38. Sayre, E. V. 1958. Studies of Ancient Ceramic Objects by Means of Neutron Bombardment and Emission Spectroscopy. Pages 153-180 in Application of Science in Examination of Works of Arts. Proc. Boston Museum Fine Arts Seminar. Museum of Fine Arts, Boston.
39. Sayre, E. V. 1963. Methods and Applications of Activation Analysis. *Annual Review of Nuclear Science* 13:145.
40. Sayre, E. V. 1972. *Advances in Activation Analysis*. Academic Press, London.

41. Sayre, E. V., A. Murrenhoff, and C. F. Weick. 1958. The Non-Destructive Analysis of Ancient Potsherds Through Neutron Activation. BNL Report 508.
42. Sayre, E. V., L. H. Chan, and J. A. Saldaff. 1970. High-Resolution Gamma Ray Spectroscopic Analysis of Mayan Fine Orange Pottery. Pages 165-181 in R. H. Brill, ed. Science and Archaeology. MIT Press, Cambridge, Mass.
43. Sokal, R. R., and P. H. Sneath. 1963. Principles of Numerical Taxonomy. W. H. Freeman and Company, San Francisco.
44. Stross, F. H., D. P. Stevenson, J. R. Weaver, and G. Wyld. 1971. Analysis of American Obsidians by X-ray Fluorescence and Neutron Activation Analysis. Pages 210-221 in R. H. Brill, ed. Science and Archaeology. MIT Press, Cambridge, Mass.
45. Tobia, S. R., and E. V., Sayre. 1973. An Analytical Comparison of Various Egyptian Soils, Clays, Shales and Some Ancient Pottery by Neutron Activation. Report BNL 18662.
46. Yellin, J., I. Perlman, F. Asaru, H. V. Micchel, and D. F. Mosier. 1978. Comparison of Neutron Activation Analysis from the Lawrence Berkeley Laboratory and the Hebrew University. Archaeometry 20:95-100.

ACKNOWLEDGMENTS

Thanks and praise be to Allah for his guidance, and peace be upon his prophets.

The author thanks King Abdulaziz University Jeddah, for their full support.

He also wishes to express his gratitude to his Major professor, Dr. D. M. Roberts, for all the great helps that he provided.

Thanks to others who have made valuable contributions to the successful completion of this work, among them, Dr. M. Glascock of the MURR.

The author wishes to acknowledge and thanks all of his colleagues with whom he shared constructive discussions and advice, among them, Mr. M. Benghanem and Mr. M. Haboub.

Finally, the author is indebted to his family for their patience and encouragement.